ADVANCED HEALTHCARE MATERIALS
www.advhealthmat.de

Multimodal Technologies for Closed-Loop Neural Modulation and Sensing

Lizhu Li, Bozhen Zhang, Wenxin Zhao, David Sheng, Lan Yin, Xing Sheng, and Dezhong Yao**

Existing methods for studying neural circuits and treating neurological disorders are typically based on physical and chemical cues to manipulate and record neural activities. These approaches often involve predefined, rigid, and unchangeable signal patterns, which cannot be adjusted in real time according to the patient's condition or neural activities. With the continuous development of neural interfaces, conducting in vivo research on adaptive and modifiable treatments for neurological diseases and neural circuits is now possible. In this review, current and potential integration of various modalities to achieve precise, closed-loop modulation, and sensing in neural systems are summarized. Advanced materials, devices, or systems that generate or detect electrical, magnetic, optical, acoustic, or chemical signals are highlighted and utilized to interact with neural cells, tissues, and networks for closed-loop interrogation. Further, the significance of developing closed-loop techniques for diagnostics and treatment of neurological disorders such as epilepsy, depression, rehabilitation of spinal cord injury patients, and exploration of brain neural circuit functionality is elaborated.

1. Introduction

Treating neurological diseases depends on the progress of neuroscience and scientific study of the nervous system that have developed in recent years facilitated by a range of innovative research methods. These methodologies include neurophysiology,[1,2] two-photon microscopy,[3,4] magnetic resonance systems,[5] optogenetics,[6] and biochemistry.[7] The development of these technologies has significantly promoted the exploration of the structure and functionality of the brain. However, conventional open-loop methods share a common limitation that their stimulation and detection capabilities deliver predefined, rigid, and unchangeable signal patterns to their targets which is unrelated to target neurophysiological signals detected. Such a limitation renders the systems incapable of adapting to the rapidly shifting dynamics of biological processes. Furthermore, open-loop control systems often require extensive time and energy to adjust to proper stimulation parameters. Currently, the main type of neural interfaces in application are primarily open-loop systems, although there are also closed-loop systems, especially electrical methods for control and monitoring.

Compared to open-loop systems, closed-loop systems have the advantage of interactivity, making them highly desirable for advancing research in the fields of neuroscience and neurological diseases. Closed-loop systems not only provide controllable stimulation to neurons but also collect and analyze real-time signals from the target, while enabling adjustments to the stimulation pattern according to the target's state. Furthermore, the feedback provided by closed-loop systems is beneficial for the plasticity of neural circuits by replacing damaged or establishing new pathways in the nervous system. A series of control techniques for achieving closed-loop control systems have emerged recently that control the latency, discharge levels, and discharge rates of neuronal action potentials, resulting in improved brain–computer interfaces[8] and induced motor plasticity.[9]

Numerous reviews on multimodal neuromodulation approaches have been published; however, few have focused on technologies for closed-loop neuromodulation and sensing.[10–13] In this Review, we discuss advancements in closed-loop neuromodulation technologies, and we specifically focus on the central

L. Li, D. Yao
Sichuan Provincial Key Laboratory for Human Disease Gene Study and the Center for Medical Genetics
School of Life Science and Technology
University of Electronic Science and Technology of China
Chengdu 611731, China
E-mail: dyao@uestc.edu.cn

B. Zhang, L. Yin
School of Materials Science and Engineering
The Key Laboratory of Advanced Materials of Ministry of Education
State Key Laboratory of New Ceramics and Fine Processing
Laboratory of Flexible Electronics Technology
Tsinghua University
Beijing 100084, China

W. Zhao, D. Sheng, X. Sheng
Department of Electronic Engineering
Beijing National Research Center for Information Science and Technology
Institute for Precision Medicine
Laboratory of Flexible Electronics Technology
IDG/McGovern Institute for Brain Research
Tsinghua University
Beijing 100084, China
E-mail: xingsheng@tsinghua.edu.cn

The ORCID identification number(s) for the author(s) of this article can be found under https://doi.org/10.1002/adhm.202303289

DOI: 10.1002/adhm.202303289

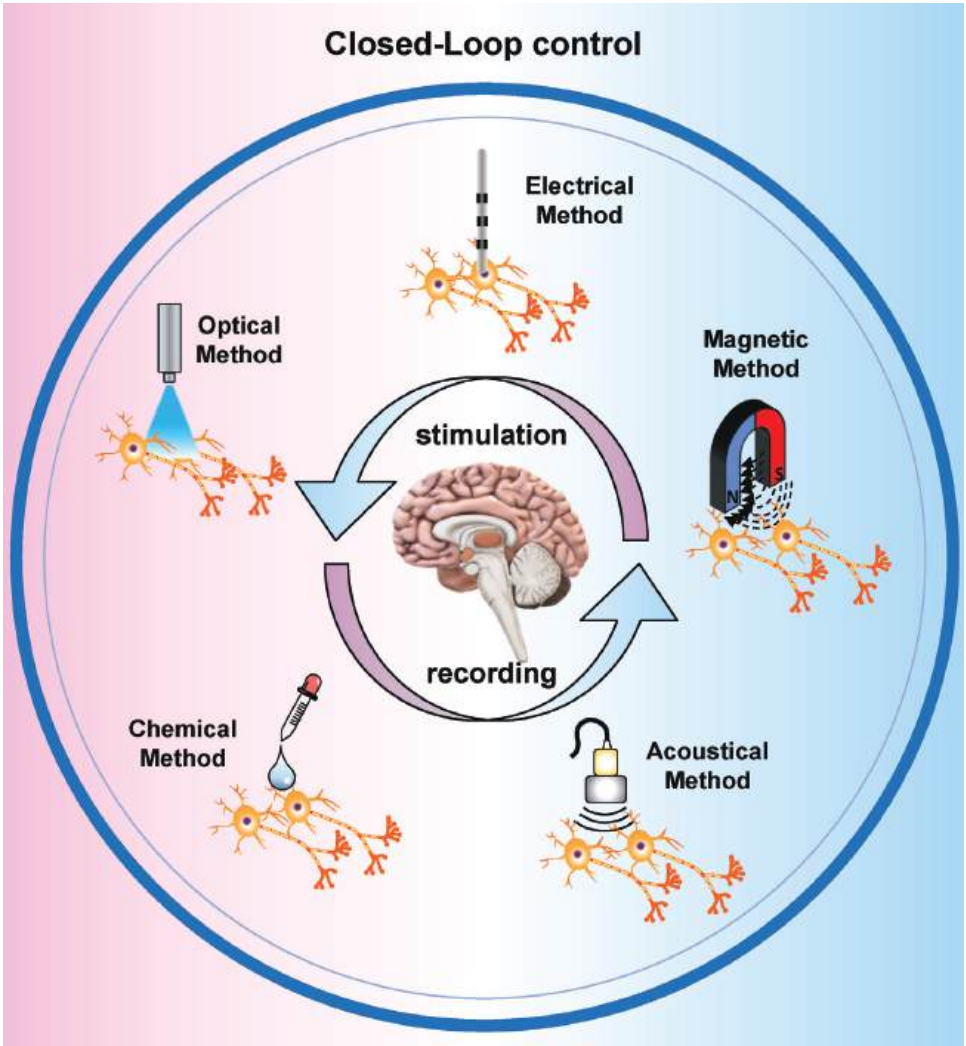

Figure 1. Schematic of closed-loop systems with multiple modalities for neurostimulation and recording.

nervous system (CNS), which plays an important role in coordinating functions such as information transmission, storage, and processing through the brain and spinal cord. The interactive regulation between the CNS with peripheral nervous system (PNS) also plays a crucial role in neuroscience research and has been discussed in the literature.[14,15]

In this review, we categorize the different technical approaches for neural stimulation and recording into several groups, namely electrode stimulation and electrode recording, optical stimulation and optical recording, electrode stimulation and optical recording, optical stimulation and electrode recording, chemical stimulation and electrode recording, electrode stimulation and electrochemical recording, ultrasound stimulation or recording, and magnetic stimulation or recording (**Figure 1**). Electrical stimulation and recording are traditional methods that can be divided into implantable and nonimplantable (wearable) approaches, which are applied widely in clinical practice. However, their nonspecificity limits their application in neuroscience. A combination of optical methods and genetics enables stimulation and regulation of a specific class of neurons, which is advantageous for studying complex neural circuits. However, the activities of neurons not only contain electrical signals but also abundant neurotransmitters, which facilitate the transport and conduction of electrical signals. Therefore, the development of a closed-loop regulatory system that considers chemical stimulation and recording is an important research topic in neuroscience. Furthermore, ultrasound and magnetic signals, which are safe and noninvasive have significant potential for application in neural modulation systems.

2. Electrical Stimulation and Recording

Neurological disorders such as epilepsy encompass a wide range of conditions that affect the nervous system, often leading to agonizing symptoms and reduced quality of life. Epilepsy is a neurological disorder characterized by recurrent and unpredictable seizures caused by abnormal electrical activity in the brain and leading to a wide range of symptoms.[16] The key features of epilepsy include seizures, recurrence, unpredictability, and diverse triggers. The disorder poses complex challenge for

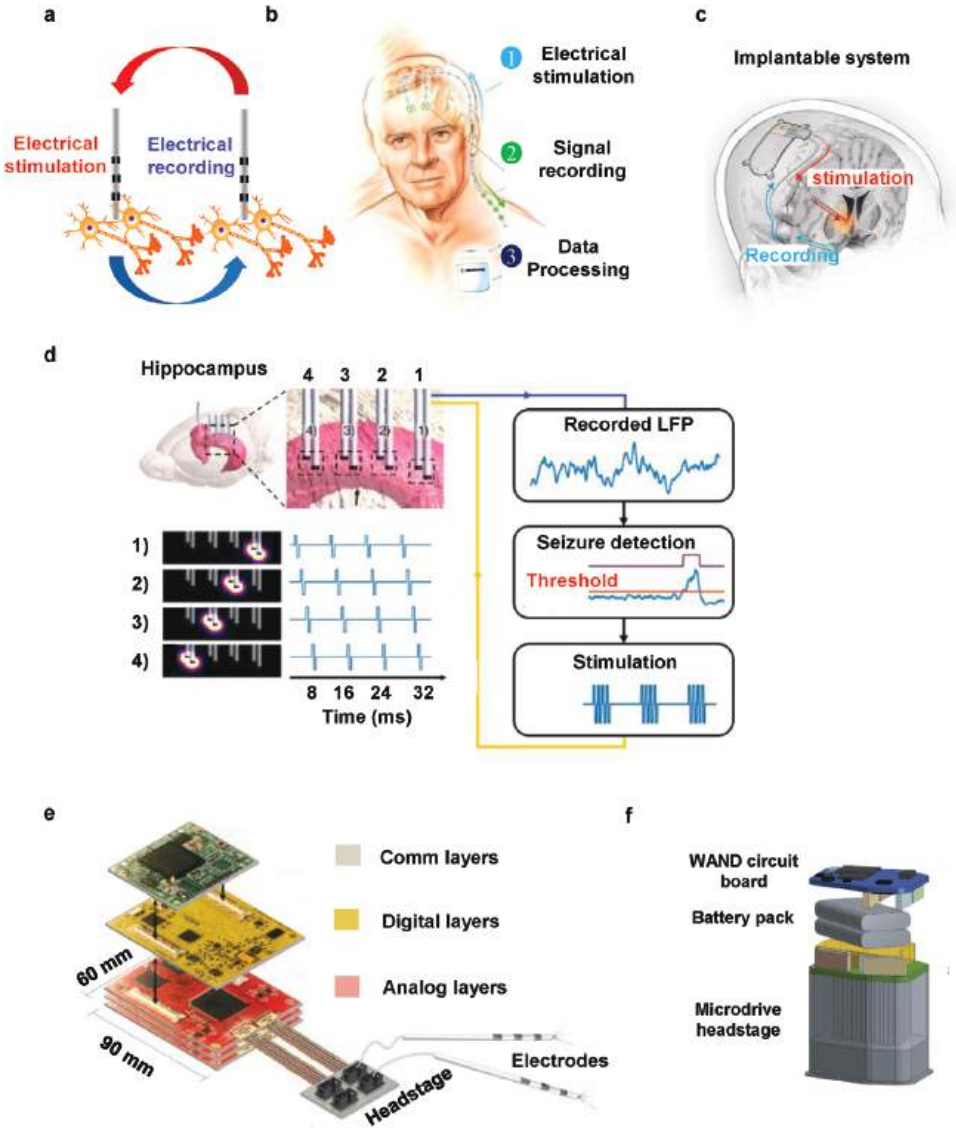

Figure 2. a) Closed-loop system with electrical neural recording and stimulation. b) Schematic diagram of Medtronic Activa PC + S system with electrical stimulation delivered to targeted areas of the brain, select brain signals detected and recorded by the system, and recorded data collected by physicians during clinical studies. Copyright: The World of Implantable Devices. c) Schematic diagram of fully implantable sensing and stimulation DBS system (Neuropace). Reproduced with permission.[29] Copyright 2021, The Authors, Springer Nature America. d) Diagram of closed-loop sequential narrow-field (SNF) stimulation system. Multichannel depth electrode arrays are inserted into hippocampal regions to record and stimulate the entire hippocampus. LFPs are used to identify abnormal brain activity in real time. Once a seizure is detected based on the setting threshold, patterned stimulation is applied to the hippocampal structure. Reproduced with permission.[30] Copyright 2022, The Authors. e) Image of the Neuro-stack PCB (size = $90 \times 60\,mm^2$), which comprises three stacked layers 1) Communication, 2) Digital layer, and 3) Analog layer. It contains ten pins (eight channels, one reference, and one ground). Reproduced with permission.[31] Copyright 2023, The Authors. f) Designed model of the wireless artifact-free neuromodulation device (WAND), with a Microdrive head stage and battery pack. Reproduced with permission.[32] Copyright 2018, The Authors, Springer Nature Limited.

clinicians seeking effective treatments. Historically, treatment options have included pharmacological interventions,[17] surgical procedures, and open-loop deep brain electrical stimulation.[18–20] With advances in neuroscience, usage of therapies delivered through implantable devices has increased significantly for assessing and treating abnormal brain activity in patients with brain disorders.[19,21] It is important to note that epilepsy is a highly individualized condition. Specific features and experiences vary significantly between individuals. Although these approaches have shown promising results in the treatment of neurological disorders, they often lack the precision and plasticity required to optimize outcomes and minimize side effects. Effective management and treatment plans have to be tailored to the unique circumstances of each individual patient.

By integrating electrical recording and stimulation into a closed-loop system (**Figure** 2a), real-time monitoring of neural signal discharges and administration of electrical therapy based on biomarker prediction offer personalized and precise treat-

ments, thereby easing symptoms and improving patient well-being. In this section, we introduce advanced closed-loop neuromodulation devices and discuss their advantages and clinical applications for various neurological disorders. Although decoding of information based on brain network signals is important, this factor is not discussed.

Activa PC+S (Medtronic, Minneapolis, MN, USA)[22] and the RNS system (The NeuroPace Responsive Neurostimulation system, Mountain View, CA, USA)[23] are two commercially available closed-loop control platforms for treating neurological diseases approved by the U.S. Food and Drug Administration (FDA). These systems continuously monitor brain activities. When abnormal neural activity indicator of an impending seizure is detected, electrical stimulation is delivered to the target to disrupt the disease cascade. The difference between the systems is that the Activa PC + S is designed to deliver monopolar stimulation and records from the same lead probe (Figure 2b), whereas the RNS includes two probes for stimulation and recording each, which are coordinated using a control circuit unit in the cranium (Figure 2c). The lead probe can be a cortical strip lead or DBS lead, depending on the location of the patient's seizure focus. Moreover, the RNS has several built-in signal-processing algorithms for closed-loop control.

The RNS system has been approved by the FDA for treating seizures in patients aged > 18 years.[24] This system includes a cranially implanted pulse generator connected to one or two in-depth and/or cortical strip electrodes placed at the location where the seizure occurred previously. Electrocorticographic (EcoG) patterns are used as biomarkers that trigger short-term stimulations. This stimulation method has been reported to reduce the frequency of partial seizures, with good tolerability and acceptable safety.[21,25]

In 2021, the RNS was used to treat major depressive disorder (MDD), a mood-related disorder with high heterogeneity in interindividual responses.[26–28] The RNS system was fully implanted in the right hemisphere (Figure 2c), and the sensing contact leads were placed in the amygdala. Furthermore, four stimulation contact leads were placed in the ventral capsule/ventral striatum (VC/VS).[29] During treatment, 6 s of stimulation was administered when an abnormal change in the biomarker was detected. This closed-loop approach rapidly alleviated both symptom severity (measured daily using the six-item Hamilton Depression Rating Scale Visual analogue scales) and depression (measured using the periodic Montgomery–Åsberg Depression Rating Scale).

Although PC+S and RNS have significant technological advancements compared with open-loop systems, they still have several limitations such as limited battery life, number of channels, and algorithms, as well as side effects. As regards side effects, Figure 2d shows a new hippocampal stimulation method called sequential narrow-field (SNF) stimulation that uses sequential tissue microstimulations, effectively terminating temporal lobe seizures while preventing edge-field effects that could cause multiple side effects. The developed closed-loop feedback stimulation system comprises recording and stimulation modules, controlled by a customized program to detect electrographic seizures in real time. When a seizure is detected, a trigger signal is delivered to the stimulation module. The effectiveness of this new epilepsy control method was demonstrated using rigorous and systematic methods, revealing the overall therapeutic effects of hippocampal stimulation. Electrophysiological responses induced by various stimulus configurations were also compared.[30]

A major trend in neuroscience is employing an increasing number of recording and stimulation channels. In 2023, a Neuro-stack was reported (Figure 2e), which is a compact bidirectional neuromodulation external device capable of simultaneously recording up to 128 channels of single- or dual-polarity intracranial electroencephalography (iEEG) from 256 macroelectrode contacts and recording 32 channels of single-polarity single-unit/local field potential (LFP) activity from 32 microelectrode contacts implanted in humans for clinical purposes during walking behaviors.[31] The recorded signal is sent to four adaptive stimulation artifact rejection (ASAR) engines that use adjacent recording channels to adaptively learn the shape of the stimulation artifact in real time. The signal-processing chain is front-end (FE) + nonlinearity correction (NLC) + ASAR, providing the ability to sense neural activity concurrent with stimulation. Therefore, the Neuro-stack provides customizable closed-loop multichannel stimulation with parameters such as pulse shape, frequency, amplitude, pulse width, interpulse interval, polarity, channel selection, and timing (e.g., phase-locked stimulation). The Neuro-stack successfully recorded LFP and iEEG activities in 12 patients with epilepsy, demonstrating its ability to record single-neuron activities during the walking process of patients and provide tailored stimulation. This capability contributes to the study of the neural mechanisms underlying human behavior and offers new hope for patients with brain disorders.[31]

The closed-loop feedback control loop formed by the electrical method also faces the challenge of electrically induced artifacts. Zhou et al. fabricated a wireless artifact-free neuromodulation device (WAND; Figure 2f), which increases the number of channels for continuously monitoring neural biomarkers to achieve wireless and artifact-free closed-loop neuromodulation.[32] The WAND comprises two custom-designed 64-channel neural interfaces; a system-on-chip (SoC) field-programmable gate array (FPGA) for flexible and reprogrammable back-end processing; a robust, bidirectional wireless link to a graphical user interface (GUI) for device configuration and control; as well as data logging. This device simultaneously supports low-noise recording and high-current stimulation.[32] When designing such devices, it is essential to integrate multichannel recording, biomarker detection, and microstimulation technologies into a single unit, with careful consideration of their interactions. The main challenge is, therefore, the substantial voltage fluctuations resulting from stimulation. These fluctuations lead to stimulation artifacts with the potential to undermine the precision of the recorded signals. By expanding the linear input range of the amplifier and increasing the tolerance to direct current (DC) offset, saturation can be prevented effectively. Additionally, the duration of artifacts can be reduced by swiftly clearing the accumulated stimulation charges from the circuit components. The neuromodulation integrated circuit employs a stimulator with high-precision charge balancing to prevent the occurrence of significant indirect artifacts while minimizing their impact on the front-end circuitry.

In the preceding paragraphs, we summarized the technical progress in closed-loop control systems comprising implantable electrical stimulation and electrical recording units in terms of device aspect. **Figure 3** shows their applications. The

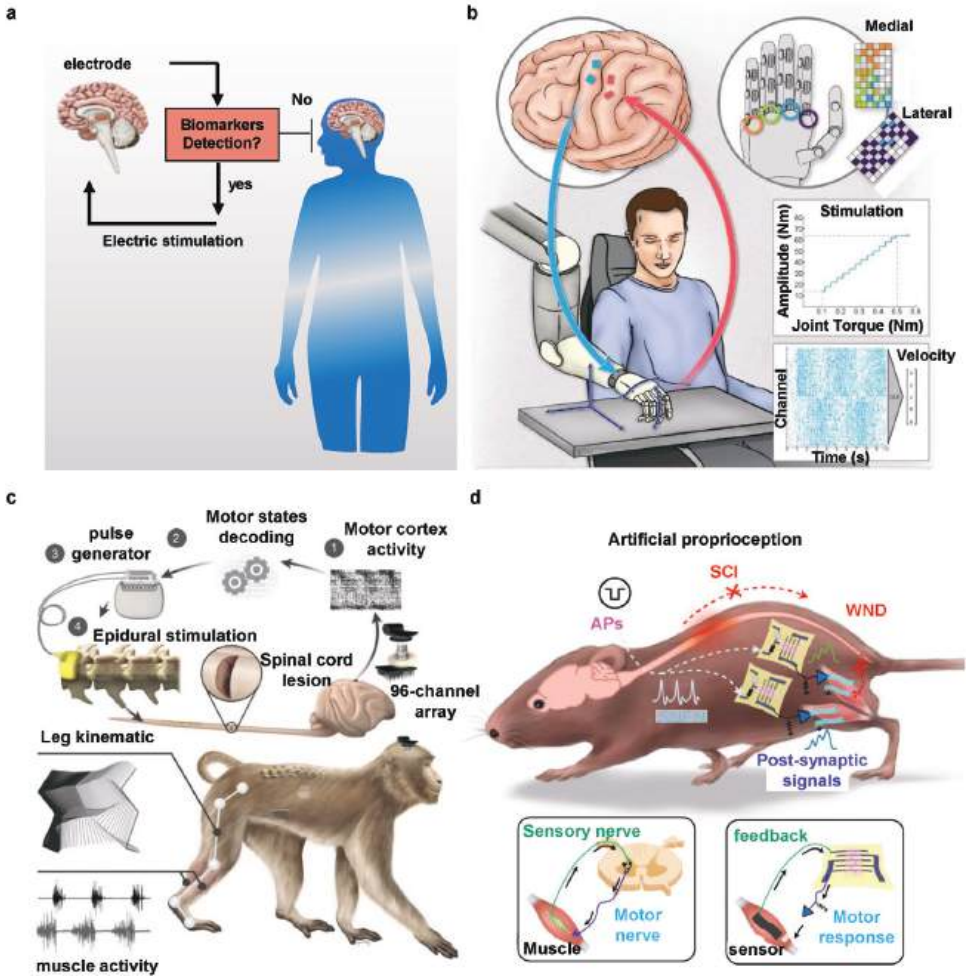

Figure 3. Various application scenarios of combining electrical stimulation and electrical recording to form closed-loop control systems. a) Schematic of the closed-loop control with electric recording and electric stimulation for treating seizures. b) Schematic of the participant bidirectional control brain–computer interfaces (BCI) to control a robotic prosthesis moved in all five dimensions in real time. Upper-left: Implanted position of the four microelectrode arrays. Upper-right: Stimulation signals evoke sensations in the robotic prosthesis. Middle-right Stimulation current amplitude modulated by figure joint torque using a linear transformation. Lower-right: Example signals recorded from the motor cortex and decoded into movement intent by an optimal linear estimator (OLE). Reproduced with permission.[47] Copyright 2021, The American Association for the Advancement of Science. c) Schematic diagram of the technical design of the brain–spine interface for primates. The monkeys were implanted with a microelectrode array into the leg area of the left motor cortex. During recordings, neural signals were transmitted wirelessly to a control computer. The closed-loop control system comprises four main modules 1) 96-channel array for recording motor cortex activity. 2) Motor states decoder for identifying motor states from neural signals. 3) Implantable pulse generator to trigger the stimulator in real time. 4) Epidural stimulation inserted into the epidural space over lumbar segments. Reproduced with permission.[48] Copyright 2016, Macmillan Publishers Limited, part of Springer Nature. d) Schematic diagram of the stretchable neuromorphic efferent nerve (SNEN) that bypasses the damaged nerves and transfers the neuromorphic electrical signals directly to the muscle as a functional replacement of the damaged nerves. Reproduced with permission.[50] Copyright 2022, The Authors, Springer Nature.

advent of closed-loop control methods combining electrode recording and electrode stimulation represents a transformative approach for treating neurological disorders, such as epilepsy,[30] depression,[29] and Parkinson's disease[33,34] (Figure 3a). Such systems have enabled adjustment of stimulation parameters in real time to control pathological brain rhythms,[35] significantly improving treatment efficiency,[36] reducing stimulus doses,[37,38] and minimizing side effects.[39,40] Clinical trials in 2013 showed that a closed-loop system, compared with traditional electrical stimulation therapy, improved patients' motor scores by 22% and reduced energy consumption by 29%.[41] The advantages of personalized treatment, minimal unnecessary stimulation, improved treatment efficiency, and enhanced patient safety make closed-loop systems promising avenues for patients and healthcare providers. With ongoing technological advancements and clinical research, closed-loop neuromodulation has the potential to revolutionize the management of various neurological conditions, ultimately improving the quality of life of countless individuals affected by such disorders.[42]

In addition, neural regulatory devices that achieve closed-loop control are important for the recovery of patients with spinal cord injury (SCI) and paraplegic walking.[43,44] For example, a closed-loop system formed by electrical detection and electrical stimulation units can be used to establish an artificial tactile feed-

back system for patients diagnosed with tetraplegia owing to SCI. Compared with brain–computer interfaces without tactile feedback,[45,46] this system significantly enhances the functional performance during grasping tasks.[47] As shown in Figure 3b, the artificial tactile feedback system implanted two microelectrode arrays with 88 wired electrodes into the brain region responsible for controlling hand and arm movements (blue dots in Figure 3b) to interpret the patient's movement intentions. In addition, two microelectrode arrays with 32 wired electrodes each were implanted into the brain region responsible for sensing skin touch (pink dots in Figure 3b), which corresponds to the skin area of the somatosensory cortex. Signals from the motor cortex control the movement of the prosthetic limb, whereas tactile signals enter the somatosensory area of the brain during movement, generating stimulation to further guide the patient's movement intentions. The addition of an artificial tactile feedback loop system reduces the time required for patients to complete tasks and significantly improves patient performance. This technology has profoundly influenced the development of brain–machine interface technology and offers new hope for individuals with SCI to regain a lifestyle similar to that of healthy individuals.

The abovementioned strategy of connecting cortical electrical activity to the sensory feedback of robotic limbs through a brain–machine interface has enabled the effective control of neural prosthetics. A similar approach can be used to control leg muscles and restore the walking function in patients. Stimulating electrodes were implanted in the epidural space of the lumbar spinal cord, and electrodes were used to detect electrical brain activity in the motor cortex of nonhuman primates.[48] By decoding movement intentions, they established a closed-loop control system at the brain–spinal cord interface to control leg movements and alleviate gait impairments in nonhuman primates following SCI. Figure 3c illustrates the design concept of the closed-loop control system. A 96-channel electrode array implanted in the motor cortex was used to record the spiking activity of the neuronal groups. The recorded signals are transmitted through wireless modules to an external receiver. After decoding the respective intentions for the extension and flexion of the muscles, stimulation signals were transmitted wirelessly to the implanted pulse generators in the epidural space, thereby controlling the implanted devices with appropriate electrical stimulation patterns. The key feature of this closed-loop control system is the association of neural electrical activity from the brain cortex with the movement patterns of the thigh muscles, enabling smooth coordination between the brain and spinal cord. Another closed-loop control system feedback signal is extracted from the mapping relationship between epidural electrical stimulation and sensory motor circuit neural regulation, as well as leg movement adjustment.[44] Based on these mapping relationships, the closed-loop control system could "automatically adjust" the electrical pulse width, amplitude, or frequency of the device within a given range, thereby achieving free movement in paralyzed rats without rapid fatigue. This system is a new approach for clinical research aimed at restoring motor function in SCI patients.[49]

However, these devices require complex circuits. And the electrical artifacts induced by microsimulation in these systems were rejected by a combination of digital signal blanking and filtering to reveal the action potentials. Here, a stretchable neuromorphic efferent nerve (SNEN) successfully induces complex and coordinated leg movements by stimulation through a soft neural interface, whereas a stretchable electronic system monitors changes in the legs in situ to avoid complex extraction and analysis calculations of biological markers. The SNEN includes organic nanowire synaptic transistors acting as biomarker extraction tools that simultaneously stimulate the target without complex controlling circuits, allowing operation at lower power levels (≈1/150 of traditional microprocessors). The SNEN controls the movement of mouse legs by bypassing damaged nerves while also having the function of preventing overtraining. Figure 3d shows the working schematic. Two different SNENs were placed in different muscles. Biomimetic action potential (AP) signals were introduced into an artificial proprioceptor and subsequently transmitted to a synaptic transistor. A carbon-nanotube strain sensor senses the muscle strain and modulates the output voltage of the artificial proprioceptor. Analog feedback-controlled presynaptic voltage pulses were controlled by the gate electrode of the artificial synaptic transistor, and the resulting postsynaptic drain output signals were employed to stimulate the leg muscles of the mice.[50] This working principle is similar to that of biological autonomous movement response, which marks a stride into the realm of future artificial neural systems. In the future, simple systems such as SNEN, which utilize the principles of neural plasticity, could signify a promising biotechnological avenue for inducing autonomous movement in organisms afflicted by motor disorders, potentially obviating the requirement for bulky and intricate electronic apparatuses.

The closed-loop regulation scheme formed by electrical stimulation and recording has been developed from the simplest single implantable electrode stimulation and recording to multielectrode adaptive stimulation and bidirectional closed-loop stimulation of a single neuron in the human body. Control circuits and algorithms have been developed for these systems; however, multiple challenges remain. For example, the lack of cell-specific targeting capabilities makes it difficult to determine how specific cells integrate into local circuits and decode local excitatory/inhibitory circuits. Additionally, it is difficult to detect and regulate chemical signals, which are important messengers in the transmission of signals in the CNS. In the future, closed-loop electrical systems could develop into systems that are less invasive with high-density recording sites. In the following sections, our focus is on the development of optics, chemistry, acoustic, and magnetism related to closed-loop control systems, which have better specificity and whole-brain detection properties, and can serve as complement of electrical methods.

3. Optical Stimulation and Recording

The study of basic neural circuits based on animal behavior is rapidly developing, with many discoveries in the past decade having been made through the implementation of fundamental technological principles, such as genetics, anatomy, and high temporal precision.[51] In this section, we focus on the development of the close-loop control systems based on optical stimulation and recording methods, which are mainly used in the field of basic neuroscience research. The electrical approaches mentioned in the previous chapter can readily be applied to the medical field. However, electrical stimulation typically involves the delivery of

an electrical current to neural tissues through electrodes, which is nonspecific, meaning that it not only activates target neurons but also potentially triggers neighboring neurons and tissues. This nonspecific stimulation could cause undesired side effects such as pain, muscle contractions, and sensory abnormalities, which limits its further application in the field of neuroscience. Furthermore, electrical artifacts from stimulating electrodes prevent precise simultaneous recording from local neurons; therefore, it is unclear whether particular brain stimulation paradigms activate, inhibit, or desynchronize the target tissue. In particular, to monitor and modulate the same local neuronal population, a closed-loop stimulation system using electrical stimulation and recording produces many artifacts associated with the electrical stimulation, limiting the expansion of the closed-loop system. Therefore, the compromising method involves restricting the control method to basic binary decisions of either "on" or "off" to prevent continuous stimulation sequences.

To avoid side effects and reduce interference artifacts between electrical stimulation and electrical recording, the stimulation can be replaced by an optical method that have high cell specificity. With the advancement of genetic encoding technology, optical techniques, such as optogenetics and fluorescence imaging, have emerged. These methods are characterized by their specificity, accuracy, and high temporal and spatial resolutions. In optogenetics, a single gene encoding a light-activated ion conductance regulator or biochemical signaling protein is introduced into target cells.[51,52] Optogenetics can perform acute or chronic excitatory or inhibitory regulations on specific neurons and is used widely in neuroscience research.[52] Fluorescence imaging technology, conversely, utilizes genetically encoded fluorescent proteins to visualize the activity of neurons and neurotransmitters through fluorescence signals.[53–56] A combination of these two techniques promotes the development of all-optical closed-loop control technology (**Figure** 4a), enabling specific stimulation of neural circuits and accurate recording of neuronal activity and neurotransmitters. Accordingly, an effective means for quantitative and precise study of neural circuit function is provided and research in related neuroscience and neurological disorders is promoted. However, due to the need for viral injection and genetic expression in both of these methods, they are currently limited to basic neuroscience research in animals.

Techniques for achieving full optical closed-loop control are relatively under explored. We have organized the development route from ex vivo to in vivo, and from traditional fiber optics to wearable and mobile technologies. Figure 4b shows a conventionally method combines fluorescence microscopy with optical stimulation systems in brain slices in vitro. Genetically encoded voltage indicators (GEVI and QuasAr2) have been used to measure the voltage-dependent fluorescence of excitable cells.[57] The light-sensitive protein BiPOLES (a tandem protein containing the depolarizer Chrimson and hyperpolarizer GtACR2) was used to provide the desired light stimulus. In this system, suitable hardware and software were implemented to excite the fluorescence of rhodopsin GEVIs. A schematic of the all-optical closed-loop control technology is shown on the right side of Figure 4b. The area of interest was monitored using a camera and the recorded signal was compared with the set target value. If the signal was lower than the threshold, the area was irradiated with orange light to control the depolarization. If it was higher than the threshold, the area was illuminated with blue light to control hyperpolarization. Therefore, this all-optical closed-loop voltage clamp system not only controls the resting membrane potential but also accurately and dynamically clamp the spontaneous rhythmic activity and high-frequency action potential of motor neurons. Although this method can only be used in brain slices in vitro, it can be extended to animal behavior and could pave the way for future therapeutic applications.

In vivo, new methods for closed-loop all-optical regulation of neuronal activity are needed in behavioral research. The connections between neural circuits can be studied directly while observing animal behavior, allowing direct testing of models of circuit connectivity, dynamics, and plasticity. However, the development of this type of system still faces many challenges, one of which is the crosstalk between the optical stimulation signal and the fluorescence signal. To overcome this problem, separate fibers can be combined for optogenetic stimulation and fluorescence detection.[58,59] Figure 4c shows a schematic diagram of an all-optical closed-loop feedback regulation system in a freely moving mouse, which combines a narrow-linewidth laser with a customized lock-in amplification scheme for coherent signal detection and noise suppression. This technique achieves coherent detection of optical signals to suppress artifacts and crosstalk between the optogenetic stimulation and fluorescence recording signals. An integrated bifurcated fiber bundle and all-fiber transmission single-channel fiber measurement system were designed, customized, and combined with a nonwavelength-selective multibranch fiber bundle with a photomultiplier (PMT). Figure 4c shows the overall structure of the bundle and the cross section of each branch. The fiber bundle contained three parts, namely a single fiber branch i), collective branch ii), and common branch (ii). Branch i was used for transmitting optogenetic excitation light and was placed at the center of branch iii, surrounded by 82 optical fibers (branch ii), which were used to collect fluorescence signals. The artifacts between the optogenetic stimulation channel and the fluorescence recording channel were reduced using the lock-in amplification method of narrow-linewidth lasers and the recording system. This all-optical closed-loop feedback regulation system supports the recording of multiple neuronal calcium activity signals and optogenetic stimulation of freely moving mice to study interactions between different neuron types and neurotransmitters in animal behavior and supports monitoring feedback effects in real time to guide optogenetic manipulation.

However, the regulatory systems introduced above, which are tied to the constraints of fiber optics, limit the study of complex animal behaviors. The integration of microscale devices with wireless circuits can relieve the constraints from the limitation of fiber optics, promising the ability to implement closed-loop feedback regulation in multiple animals. This thus provides a powerful tool for studying complex social behaviors. A combination of micro-LED probes and fiber photometry [58] (Figure 4d) provided an opportunity to regulate dopamine release. In the current study, ChrimsonR and stGtACR2 were used for bidirectional control of neuronal activity in the ventral tegmental area (VTA). We used DA2m (a new, improved extracellular dopamine indicator) to detect the amount of released dopamine.[60] This device can potentially be developed into a closed-loop control system to maintain dopamine at target levels.

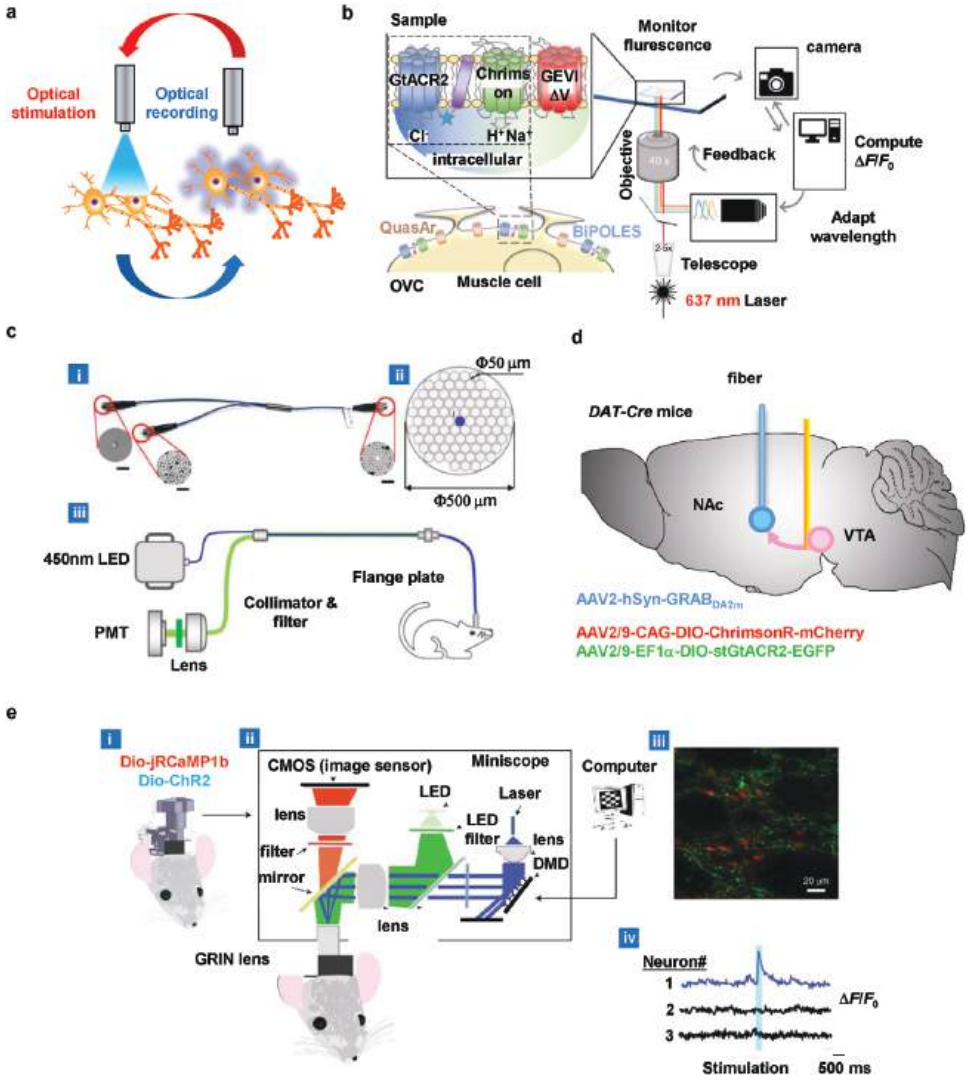

Figure 4. a) Closed-loop system with optical recording and optical stimulation. b) Molecular components of the optogenetic voltage-clamp system comprise two complementary optogenetic actuators for inducing both hyperpolarization and depolarization (GtACR2 and Chrimson, denoted by the blue star alongside mCerulean), alongside a voltage indicator. Diagram on the right illustrates the hardware setup and communication flow, with membrane voltage continuously monitored by a fast and highly sensitive camera (either sCMOS or EMCCD), and grayscale values being processed by real-time control software. The system maintains voltage stability by adjusting the light output from a monochromator to the optogenetic actuators based on the difference from the predefined holding value. Reproduced with permission.[57] Copyright 2023, The Authors. c) Custom-designed bifurcated fiber bundle and all-fiber-transmission single-channel fiber photometry system. i) Image of the bifurcated fiber bundle that comprises three branches, namely a single-fiber, collection, and common branches. The image of a branch is captured by directing high-intensity excitation light into the single-fiber branch. Scale bar, 200 μm. ii) Illustration of the common branch of the bifurcated fiber bundle. iii) Schematic representation of the single-channel fiber photometry system, designed with a custom bifurcated fiber bundle for all-fiber transmission. Abbreviations: PMT, photo multiplier tube; LED, light emitting diode. Reproduced with permission.[59] Copyright 2020, CC BY license. d) Diagram illustrating the viral injection followed by implanting the micro-LED probe for stimulation and optical fiber for photometry of DAT-cre mice. Reproduced with permission.[60] Copyright 2022, The Authors. e-i) Illustration of the placement of all-optical Patterned Stimulation and Imaging (MAPSI) on a mouse's head. ii) Schematic of MAPSI components. There are two light sources in the excitation path: an LED for exciting jRCaMP1b and a blue laser light for exciting ChR2. Micromirrors on the DMD reflect a collimated laser beam, generating arbitrary stimulation patterns that are created and controlled by a computer. Calcium activity is recorded in the emission path using a CMOS sensor. iii) Histological image displays dSPNs (D1-cre mouse) coexpressing jRCaMP1b and ChR2. iv) Calcium transients, indicating the excitation of stimulated neuron #1, while neighboring neurons #2 and #3 remain unaffected. Reproduced with permission.[62] Copyright 2022, The Authors, Springer Nature Limited.

The development of neuroscience is inevitably inseparable from that of integrated optical imaging technologies, which enabled visualization of the activities of neuron groups. In 2018, scientists achieved all-optical real-time closed-loop control by combining a genetically encoded calcium indicator, GCaMP6, and an optogenetic actuator, C1V1.[61] They obtained the raw signal in real-time from a microscope and reconfigured the optical stimulation strategy through integrated hardware after online analysis. These scientists achieved an all-optical "activity clamp" to maintain an individual neuron at a target activity level to enhance the sustained sensory-evoked activity patterns in individual neurons in an awake mouse. In addition, the closed-loop control method can correlate trigger neurons with target neurons to flexibly control the temporal and spatial patterns of neural circuit activity.[61] In 2022, scientists developed a one-photon system to achieve all-optical modulation, namely the Miniscope with All-optical Patterned Stimulation and Imaging (MAPI). The instrument was integrated into a small device with functionalities such as pattern stimulation and calcium recording (Figure 4e).[62] Closed-loop experiments were performed with the miniscope, which successfully mimicked natural physiological patterns to maintain and shape real-time neural activity.[62] The difference between this technique and the previous work reported in this review is the integration of the hardware. In previous animal experiments, the mice were fixed, whereas in this scenario, freely moving mice could be manipulated, and any targeted neurons could be recorded. Therefore, the system provides higher portability and cost efficiency, offering a powerful tool for understanding the neural basis of behavior in neuroscience research.

The all-optical closed-loop control method enables flexible manipulation and positioning of neuronal activity. In the future, various gene-encoded sensors and optogenetic probes could be employed to achieve multiple detections and control in various neuron populations by selectively expressing a wide range of sensors and actuators. In addition, with the development of genetically encoded calcium, voltage sensors, and optogenetic opsins, the speed of online feedback loops would increase further in the future. Such advantages would further expand the applications of all-optical closed-loop regulation, such as correcting abnormal activity patterns in epilepsy and Alzheimer's disease. In conclusion, the all-optical closed-loop system provides a new perspective for optical brain–machine interfaces.

4. Combining Optical and Electrical Methods

All-optical closed-loop regulation has the advantages of specificity and precision, but it cannot completely replace the technology of electrical stimulation or recording, as high-resolution optical stimulation or recording techniques have not yet been achieved. Furthermore, due to the broad spectral response of opsins, optical crosstalk may exist, making it difficult to stimulate and record multiple different types of neurons simultaneously in the same region. In this section, we introduce a closed-loop system combining optical and electrical methods. A combination of these methods has significant potential for controlling the feedback with minimal artifacts. Light stimulation patterns are guided by the real-time results of ongoing electrophysiological activity monitoring, facilitating continuous, dynamic interactions with the neural tissue in real time.[63,64] This factor indicates that combining electrophysiological recording and optical stimulation methods could enable continuous and closed-loop modulation of local neural circuits without affecting the electrode records when optogenetic stimulation is applied (**Figure 5**a).

Fiber optics is employed widely in neural interface technology, typically utilizing optical transmission to convey external light signals to specific regions of the brain, thereby facilitating its application in optogenetic research.[65] To combine the electrode with the optical component, traditional hot-drawing technology for producing optical fibers is a good strategy. Because the materials that make up the prefabricated parts must be heated together during the drawing process, the selected polymers, metals, and composite materials must have sufficiently low viscosities and similar glass transition and melting temperatures. Considering the above, the materials selected for the preform could be polycarbonate (PC), cycloolefin copolymer (COC), conductive polyethylene (CPE), polyphenylene sulfone (PPSU), polyetherimide (PEI), and low-melting-point metals such as tin (Sn), rather than the conventionally used materials in optical fibers and glass. At first, the polymers, metals, and composite materials were integrated together to fabricate the preform. Employing hot-drawing technology, the preform can be drawn into multifunctional interfaces with photogenetic stimulation, neural recording, and drug delivery functionalities.[66] Figure 5b shows the drawing process and the cross-sectional geometry of the annealed-drawn flexible fibers. One multifunctional design included a cylindrical waveguide, two microfluidic channels, and two electrodes. Another is a thinner concentric design that integrates a microfluidic channel, four electrodes, and a surrounding waveguide. A concentric circular structure can reduce the size of the fibers and increase the number of recording sites. These probes achieved neural recording and simultaneous optogenetic stimulation with fewer foreign body reactions and reduced chronic astrocyte and microglial responses, allowing for stable brain–machine connectivity for two months. The results show great promise for the closed-loop control of optogenetic stimulation integrated with electrode recordings.

Understanding the precise influences of neural circuits on behaviors ranging from learning to social performance requires the ability to record multiple channels of electrical activity simultaneously when optogenetic manipulation is applied. Figure 5c shows the device design combining electrode recording and optical stimulation based on fibers (diameter 200 μm), which were rigidly equipped with sixteen microwires (polymer-coated nickel-chromium) wound into four tetrode bundles (diameter 25 μm).[67] The 16 microwires were 300–1000 μm longer than the fibers to ensure consistent and sufficient light intensity near the recording sites. In addition, this device has a superior mechanical design, combining an optical fiber and four-stage components with customized coaxial mechanical drivers to control the recording sites after implantation. This device is small and sufficiently light (weight 2 g) for application to freely behaving mice. The device explored the effects of light stimulation on neural activity in the medial prefrontal cortex (mPFC) in an open field test and during different behaviors of freely moving mice. Further, it monitored the changes in neuronal activity in specific neural projection circuits under light stimulation. Employing the device for behavioral analysis facilitates minimizing of the subjective factors of individuals.

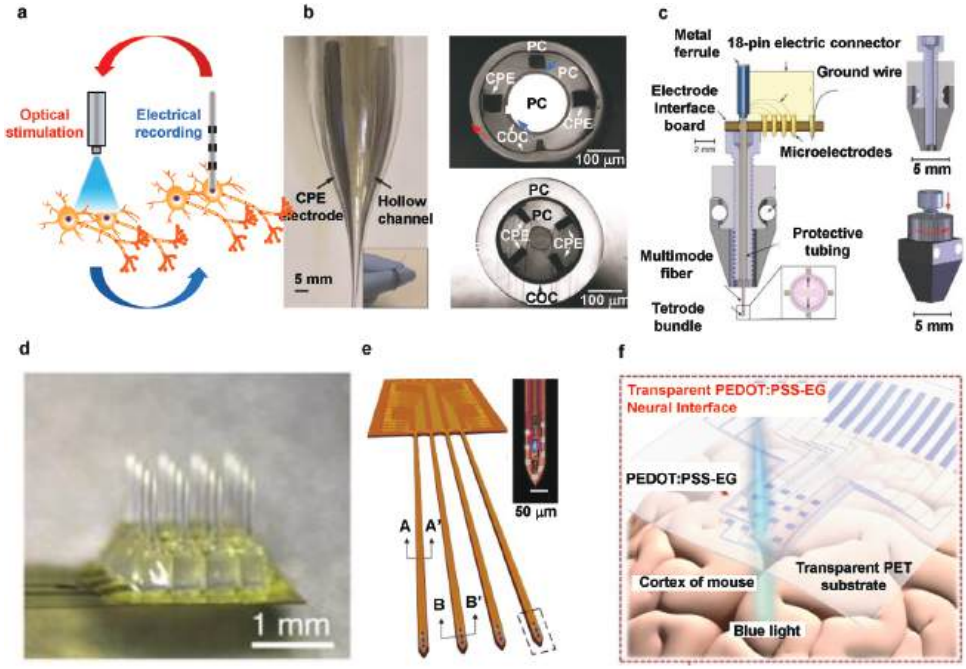

Figure 5. a) Closed-loop system with electrode recording and optical stimulation. b) Photograph of the fabrication process of multifunctional fibers. Inset: wrapped fiber around the finger. Right optical images show a cross section of fiber tips: design I (which incorporates a cylindrical waveguide, two microfluidic channels, and two electrodes), and design II (which integrates one microfluidic channel, four electrodes, and a surrounding waveguide) multimodality probe tips. Reproduced with permission.[66] Copyright 2015, Springer Nature, America. c) Schematic of cross section of the optetrode. The device comprises plastic housing and a securely fastened thumbscrew, firmly anchored by two friction-fit plastic pins. This thumbscrew serves as the mechanical driver for a perforated screw, which houses a protective tube, which, in turn, houses four tetrodes and a multimode fiber, all securely bonded together. At the opposite end of this screw, an epoxy connection links it to both the metal ferrule optical connector tip of the fiber and an electronic interface board. This interface board facilitates the connection of the tetrode microwires to an 18-pin electrical connector. In the inset, a horizontal cross section view reveals the optical fiber with its four tetrode bundles securely affixed. Reproduced with permission.[67] Copyright 2011, Springer Nature, America. d) Optical image of a 4 × 4 transparent, electrically conductive ZnO MOA device flip-chip bonded on thin, flexible, and semitransparent polyimide electrical cable for multichannel intracortical neural recording and optical stimulation. Reproduced with permission.[69] Copyright 2015, Springer Nature, America. e) Schematic illustration of a miniSTAR µLED optoelectrode, crafted using microfabrication techniques borrowed from the methodology employed in creating the family of Michigan optoelectrodes, including the one-metal-layer µLED optoelectrodes. Reproduced with permission.[70] Copyright 2020, The Authors. f) Schematic illustration of the transparent electrode fabricated by PEDOT:PSS-EG that enables conformal contact with the brain. The transparent sensing site can penetrate 473 nm blue laser so as to direct toward the target electrode. Reproduced with permission.[77] Copyright 2021, The Authors, published by Wiley-VCH GmbH.

However, because of the direct physical integration of optical fibers and electrodes in this device, the physical size of the tip of the probe is large, and a mismatch between the optical transmission position and the electrophysiological recording site cannot be avoided during the implantation process.[68] Therefore, the optrode and electrical electrodes were fabricated together using device micromachining to avoid spatial mismatches. Zinc oxide (ZnO) exhibits high conductivity, optical transparency, and biological friendliness. Through patterned metal evaporation, precision mechanical procedures, and multistep chemical etching processes, a Utah electrode array with optical transparency and high conductivity integrated with a optoelectrical stimulator and detector was fabricated,[69] as shown in Figure 5d. Acute experiments in living animals have demonstrated the ability of the device to perform optical neural modulation and low-artifact synchronous electrophysiological recordings in vivo. This development provides exciting prospects for basic and applied research, such as the development of neural prostheses and dynamic maps of deep anatomically specific neuronal populations through feedback-controlled stimulation.

Although combining optical fibers with recording electrodes is simple, the recording and stimulation sites are limited to the tip of the fiber. The Michigan electrode is another electrode array widely used in acute and chronic in vivo cellular electrophysiology and is a silicon-based multielectrode array structure. A new Michigan electrode with a high-density recording electrode array integrated with a micro-LED stimulation light source was fabricated.[70–72] Figure 5e shows one of a miniSTAR (Great Lakes Dental Technologies, New York, USA) micro-LED photoelectrodes with fewer stimulation artifacts. This structure introduces a multimetal layer structure with a shielding layer to effectively suppress the capacitive coupling of the stimulation signals. The substrate is made of heavily boron-doped silicon to suppress the diffusion of optically generated electron-hole pairs, thereby eliminating the stimulation artifacts produced by the photovoltaic effect of LED lighting. A micrograph of the probe tip is shown in the upper-right corner of Figure 5e. The sizes of the LED and recording electrodes are 10 × 15 μm^2 and 11 × 13 μm^2, respectively. The entire photoelectrode could be assembled on a printed circuit board, achieving high spatial- and temporal-

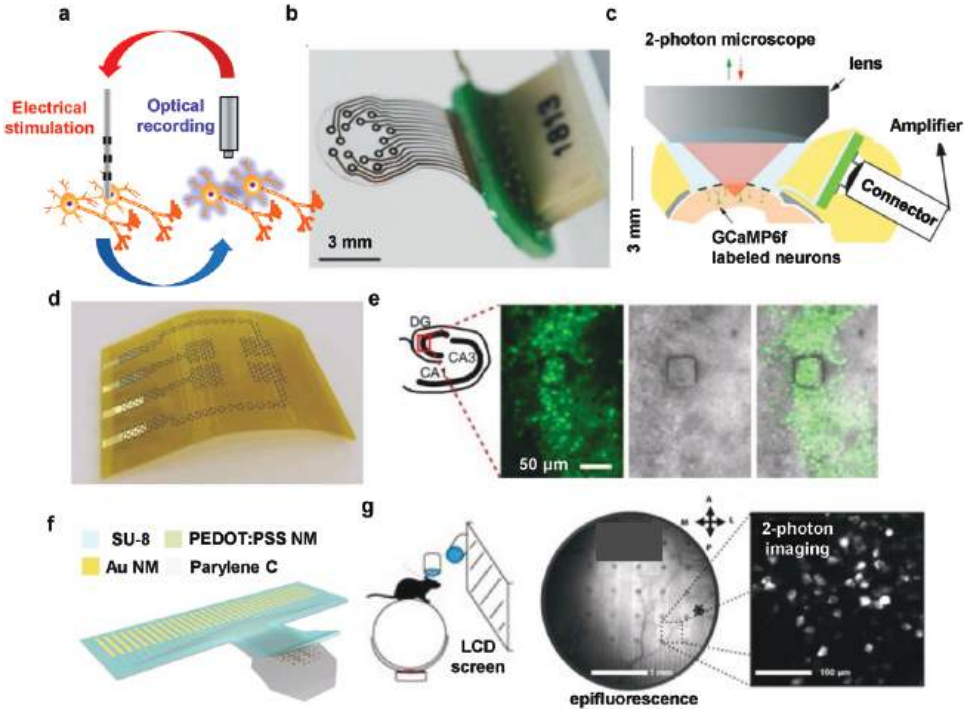

Figure 6. a) Closed-loop system with electrode neural recording and electrode stimulation. b) Photograph of the ECoG array. c) Schematic cross section of the device implanted on the mouse, illustrating imaging well and placement of connector to facilitate access of microscope objective. Reproduced with permission.[85] Copyright 2020 WILEY-VCH Verlag GmbH & Co. KGaA, Weinheim. d) Schematic illustration of a flexible graphene neural electrode array. Patterned graphene electrodes are in contact with Au contact pads to interface with the data acquisition system. e) Left schematic shows different regions of the hippocampus. The dentate gyrus is imaged by the confocal microscope. Images show left: a steady-state fluorescence (F0) image of dentate gyrus in an OBG-1 AM-stained hippocampal slice obtained through the $50 \times 50\,\mu m^2$ graphene electrode. The graphene electrode is seen as a square outline with dark edges. Middle: simultaneously obtained transmittance image. Right: merge of the steady-state fluorescence (right) and transmittance images (left). Reproduced with permission.[87] Copyright 2014, Springer Nature. f) Device schematic of the 32-channel Au/PEDOT:PSS nanomesh MEA. g) Head-restrained awake mouse on a floating Styrofoam ball, watching visual stimuli. The right figure shows wide-field epifluorescence of the visual cortex and the surrounding areas. The asterisk indicates the binocular area of the visual cortex. Reproduced with permission.[88] Copyright 2018, The Authors, exclusive licensee American Association for the Advancement of Science.

resolution recordings of neuronal activity signals and real-time driving of LEDs. The spiking activity is triggered in a neighboring neuron by a light pulse. In vivo and in vitro studies have verified that this probe could effectively suppress stimulation artifacts, allowing an in-depth study of the interactions between multiple components of neuronal circuits.

For cortical EEG recording and optical stimulation, traditional materials such as gold or platinum can be used to fabricate mesh-structured electrodes with high light transmittance. However, such materials produce artifacts in the electrophysiological data when exposed to light. Direct fabrication of transparent electrodes is a simple and feasible method.[73] By utilizing the properties of transparent electrodes, the light used for optogenetic stimulation can be transmitted to the target location.[74–76] Diverse materials are used for transparent electrodes, such as highly conductive materials soaked in ethylene glycol and poly(3,4-ethylenedioxythiophene) polystyrene sulfonate (PEDOT:PSS).[77] The working schematic is shown in Figure 5f. The development of transparent electrodes has achieved high-fidelity neural recording in the most convenient way, providing more possibilities for neuroscience research in closed-loop systems.

The integration of optical stimulation modalities with electrical recordings also faces certain challenges because of the generation of optical artifacts (**Figure 6a**). The following summarizes the development of transparent electrodes that do not block the transmission of stimulated light. There are numerous works reporting transparent electrode arrays for the neuroscience application, based on transparent organic electrochemical transistors (OECTs), Au grid wirings,[73] metal nanowires,[78–80] carbon-based materials (carbon nanotubes and graphene),[81,82] conductive polymers (CPs),[83,84] etc. Figure 6b shows the flexible, stretchable, and optically transparent 16-channel cortical ECoG array.[85] The ECoG array was created using polydimethylsiloxane (PDMS) as a substrate and employed an innovative push-through method that combines gold nanowire (Au NW) tracks with platinum (Pt) particle electrodes. The device has good compatibility with various optical and electrical readouts, such as wide-field and two-photon calcium imaging (Figure 6c). Combined with two-photon calcium imaging, neurons can be imaged near the ECoG recording electrodes (within a lateral distance up to 200 μm and depth up to 180 μm), implying it could capture high-resolution single-cell activity from several hundred micrometers below the cortical surface. This device also has high temporal resolution and multichannel ECoG recording capability.

Graphene is another potential candidate for fabricating transparent electrodes, with several studies having reported using

graphene as a transparent electrode.[86,87] The device shown in Figure 6d allows simultaneous optical imaging and electrophysiological recording. When the transparent graphene electrode is combined with confocal and two-photon microscopy to image hippocampal slices, it can capture high-frequency neuronal activity and slow-changing synaptic potentials without introducing any optically induced artifacts into the optical images, as shown in Figure 6e. Transparent graphene microelectrode technology coupled with optical imaging techniques provides a practical tool for studying neural activity across multiple spatial scales—from single neurons to large neuronal populations.

The development of transparent electrode arrays has enabled simultaneous electrical stimulation and optical imaging.[73,78–84] What's more, with the advancement of technology, improving the spatial and typological resolutions of the electrodes is a direction for future enhancement. The use of poly(3,4-ethylenedioxythiophene):poly (styrene sulfonate) (PEDOT:PSS) can potentially extend the recording resolution of transparent electrodes scale up to the level of individual neurons. Because the impedance and charge injection performance of PEDOT:PSS exceed those reported for graphene electrodes. Figure 6f shows a 32-channel Au/PEDOT:PSS nanowire microelectrode array fabricated on a flexible poly(ethylene terephthalate) (PET) film.[88] This array exhibits excellent optical transparency and mechanical flexibility. It comprises a 10-µm thick PET substrate, 25-nm thick Au nanowire microelectrodes, 85-nm thick PEDOT:PSS, and an 8-µm thick SU-8 layer for encapsulation. This device achieves precise recording of up to 200 µV signal with an error margin of approximately 20 µV, resulting in a signal-to-error ratio of 100 000 times. Figure 6g illustrates the combination of high-performance transparent arrays using Au/PEDOT:PSS bilayer nanowire microelectrodes and optical imaging technology, enabling parallel electrophysiology and two-photon imaging. In an in vivo test, a mouse expressing the GCaMP6s protein was head-fixed on a floating polystyrene foam ball, but with freedom to move. Visual stimuli were presented to the mouse through an LCD screen, and calcium activity was imaged. The plot on the right side shows the imaging results. The transparent electrodes have relatively low optical losses in the spectrum of interest, and the fluorescence signals of brain regions underneath them maintain about 73% of those in the cortical area without electrodes. This electrode facilitates high-fidelity, highly specific neural recordings and selective stimulation and can be applied widely in neuroscience and medical practice.

The development of optogenetics electrodes is a good foundation for the development and application of closed-loop systems in biomedicine. In Figure 5, the focus is on the application of closed-loop systems. A typical application is the identification and treatment of epilepsy. As mentioned previously, epilepsy can occur as recurrent and spontaneous seizures, which significantly interfere with the daily lives of patients. When a seizure occurs, the patient's level of consciousness decreases immediately, and abnormal EEG signals are distributed widely in most parts of the brain. Clinical trials using closed-loop electrical stimulation have demonstrated promising therapeutic effects. However, the incidence rate of epilepsy is extremely high, and the electrode strategy usually has no effect on the treatment of head-trauma-induced seizures.[89,90] Therefore, it is necessary to identify the relevant neural circuits that induce epilepsy and control epileptic seizures through regulation.[91] Furthermore, the types of neurons in the vicinity of epileptic lesions are complex and include excitatory and inhibitory neurons.[92] It is not possible to selectively activate epilepsy-related thalamocortical neurons using electrodes. Optogenetic stimulation affects specific cell groups in a spatially restricted manner. Therefore, optogenetic stimulation can activate the target neuron type with high accuracy and selectivity. On-demand activation of cerebellar parvalbumin-expressing Purkinje cells inhibits ongoing epileptic seizures.[93] **Figure 7a** shows the workflow for organizing spontaneous epileptic seizures using a closed-loop system with integrated electrical detection and optogenetic stimulation.[94] First, a detection electrode was used to monitor the neuronal activity in the thalamic cortex after cerebral cortex injury. The electrode was connected to the injured epileptic cortex, and customized software was used to monitor changes in the EEG. Biomarkers of epileptic seizures include signal power (amplitude and rate of change), spike (amplitude and width), and frequency (energy changes in a specific frequency band). After detecting the characteristic signals of epileptic seizures, specific wavelengths of light are used to stimulate the dorsal brain area of the hippocampus, which expresses photosensitive proteins. The study indicated that inhibiting excitatory cells or activating inhibitory cells through optogenetics could immediately interrupt electrographic and behavioral seizures and restore normal neuronal activity.[92] This finding indicates that optogenetics can be used to treat epileptic seizures with cell population specificity, limited spatial range, and shorter stimulation times, thereby reducing the side effects caused by stimulation and providing guidance for clinical research.

Additionally, a closed-loop system formed by specific optogenetic stimulation and electrical detection can be used widely in the peripheral nerves of the spine. A typical application is the recovery of the walking function in patients with SCI. Figure 7b shows a soft, stretchable, and wireless mouse spinal cord closed-loop stimulation system integrated with micro-LEDs.[95] The mouse head-mounted platform precisely controlled the pulse current of the two LEDs and obtained real time recordings of electromyographic activity from four pairs of electrodes chronically implanted in the tibialis anterior muscles. Automated photostimulation is delivered to the caudal lumbar spinal cord when new electromyographic activity is detected in the tibialis anterior muscle. The control algorithm running on the mouse head-mounted platform can automatically trigger a brief single-pulse stimulus, allowing an ultrafast closed-loop control system for light stimulation to alter mouse behavior. This system achieved closed-loop control of the entire spinal cord in an untethered and unrestricted mouse, providing a new method for treating peripheral nerve injury.

In addition, optogenetic methods have been applied in the treatment of other neurological diseases such as depression[96] and chronic pain.[97] Accordingly, optogenetics has great potential for clinical trials, although it still faces several significant barriers, such as the need for genetic transfection and light illumination. Clinical trials have begun to evaluate the safety of photosensitive proteins in the treatment of patients with neurological deficits.[98] The promotion of optogenetic probes combined with electrodes in clinics would lead to the widespread development of medical devices for patients with neurological diseases.

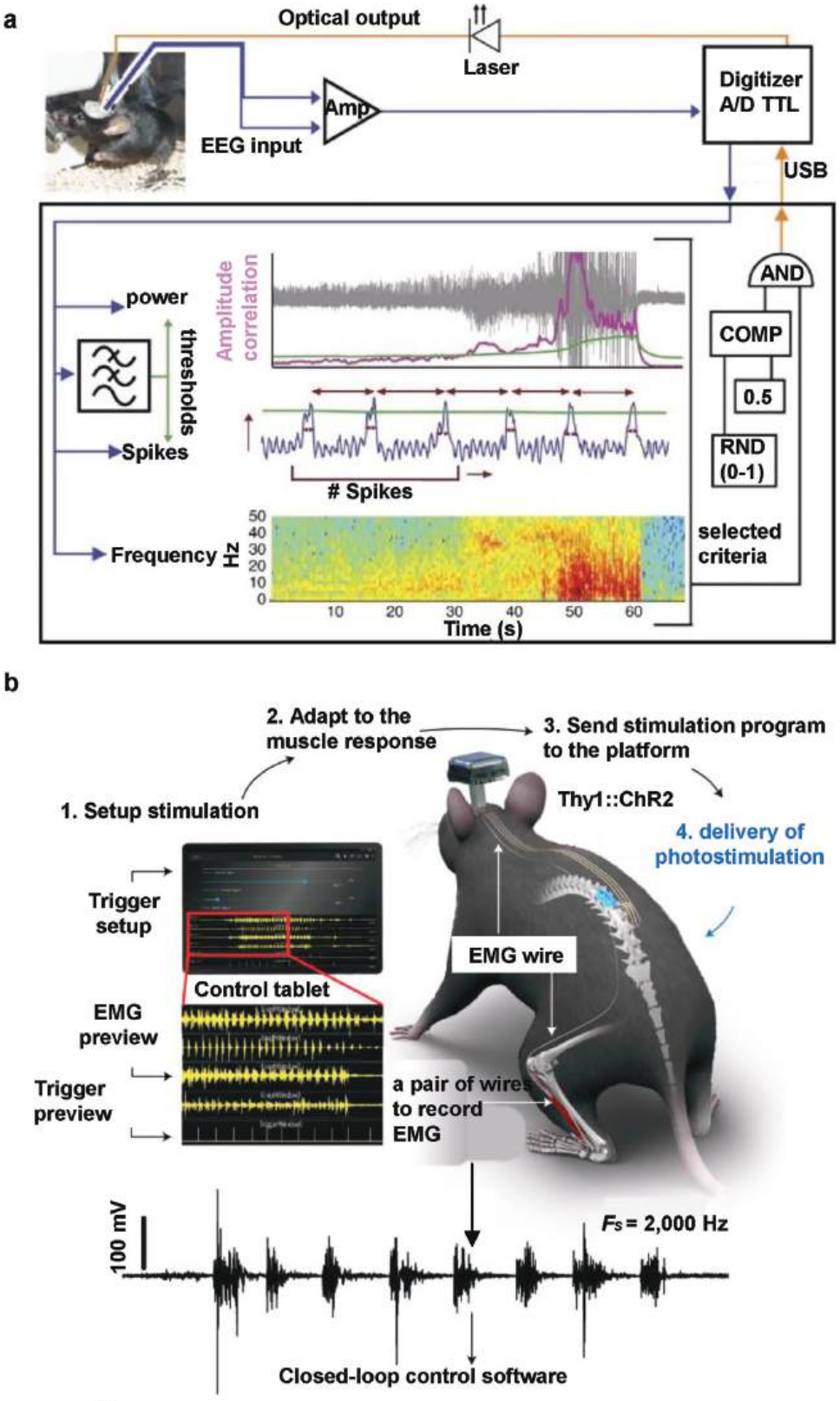

Figure 7. Various application scenarios of combining optical stimulation and electrical recording to form closed-loop control systems. a) Closed-loop system design to identify and rapidly respond to seizures. EEG input data (depicted in blue) obtained from a mouse hippocampus undergoes amplification (Amp) and digitization (A/D) before being transmitted to a personal computer running custom-designed real-time seizure-detection software.

5. Chemical Stimulation and Electrical Recording

The neural system is complex and based on complex interactions between cells, various neurochemicals, and numerous biochemical reactions. Electrical signals is one of the external effects of a complex system and can only carry partial information on neural activities, which limits modulation based only on electrical signals in chemical specificity and interpretability. Sensing and manipulation of chemical conditions of neural tissues can offer neuromodulation with high cell-specificity and more precise dosage control. Efforts toward closed-loop chemical-specific modulation systems have been made, with some studies having achieved closed-loop control and others having provided effective sensing and stimulation methods. Both are introduced in the following sections as references for the design of future closed-loop chemical neuromodulation devices.

These chemical-specific methods can generally be categorized into two types, namely specific sensing of targeted chemicals and direct stimulation of specific biochemical processes. Specific sensing focuses on monitoring the content of a substance of interest (e.g., a specific neurotransmitter) and preventing the effects of interferents. Specific binding methods, such as biorecognition are used conventionally in these techniques. Photometry is an example of chemical-specific sensing that uses fluorescent proteins as the binding agents. Similarly, the specific control of optogenetic opsins by light is an example of specific stimulation. These techniques focus on manipulating specific components of the nervous system such as membrane proteins and neurotransmitters. As drugs can directly affect specific biochemical processes, drug delivery is the mainstream in chemical stimulation. However, devices with both chemical sensing and stimulation functionalities have seldom been reported. Therefore, we discuss these separately in the following two sections.

This section focuses on modulation devices for chemical stimulation, whereas the sensing modules are based mostly on conventional electrical recording (**Figure 8a**). Because closed-loop strategies are similar to the electrical recording devices discussed in Section 2, this section mainly discusses how to achieve chemical stimulation and electrical recording in one device, i.e., how to integrate drug delivery and electrophysiological functionalities. It is noteworthy that because few drug-delivering devices have achieved actual closed-loop control, studies that only achieve independent electrical recording and drug delivery are introduced here, which could serve as references for future closed-loop devices. When combined with an appropriate control strategy, these devices can potentially achieve closed-loop modulation.

Closed-loop devices with drug delivery functions are promising candidates for the preventive treatment of hard-to-predict acute diseases such as epileptic seizures and strokes. Compared with electrical stimulation, the basic mechanism of which remains unclear, pharmacotherapy is more reliable for treatment, and closed-loop drug delivery can further increase its relevance. Theoretically, a closed-loop device loaded with a drug can be chronically implanted at a risk point, continuously monitoring neural activity. Upon disease onset, the device detects abnormal signals and initiates drug delivery, thereby providing immediate treatment. This strategy significantly reduces the interval between disease onset and treatment, thereby increasing the possibility of cure. This concept was proven in a rat model using a multifunctional device with EEG monitoring, drug delivery, and closed-loop control.[99]

To develop devices with both electrophysiological recordings and neurochemical stimulation functionalities, several researchers have integrated electrodes for recording with microfluidic channels for drug delivery. Microfluidic channels can be connected to a back-end drug injection system to achieve convenient drug delivery upon request. Microfabrication procedures are used to fabricate more finely defined and compact devices that combine electrodes and microfluidic channels. Several research groups have developed microfabrication processes to achieve modulation devices using metal electrodes and built-in microfluidic channels made of silicone or polymers.[100] For example, Cho et al.,[92] fabricated an 80-µm-thick, 40-µm thick neural probe with microelectrode array for electrophysiological recording and a microfluidic channel for drug delivery out of silicon employing microfabrication.[100] The probe was implanted into the thalamus of mice, where the microfluidic channel delivers pilocarpine to induce seizures and electrodes record neural activities associated with the seizure events. Based on this achievement, the same research group further developed a multishank neural probe with extra functionalities for recording neural activity at more sites and transmitting light through an SU-8 waveguide[101] (Figure 8b). Combined with a control system that considers the feedback of electrophysiological signals, these devices have the potential to achieve closed-loop regulation.

Several strategies can be used to fabricate microfluidic channels using microfabrication. Photoresist can be used as a sacrificial space holder, removed, and as microfluidic channels when other components including electrodes and encapsulation are formed. Song et al.[102,103] used a photoresist layer to form a space-holding sacrificial structure by photolithography, deposited parylene to form channel walls, and then removed the photoresist using acetone to produce the parylene-based microfluidic channel. The devices were implanted in the sciatic nerves of rats and could obtain electromyography (EMG) signals and deliver the dye. Lee et al.[104] used a similar strategy with an AZ sacrificial layer and polybenzocyclobutene channel walls to fabricate a device that was used in the neural recording of the barrel cortex of rats. Microfluidic channels can also be obtained by sealing an etched silicon trench by binding a wafer to another silicon substrate or by the deposition of silicon dioxide. Seidl et al.[105] fabricated a probe with a microfluidic channel by direct wafer

This software employs various detection algorithms, such as signal power, spikes, or frequency. Once a seizure is identified based on the chosen criteria, the software activates the optical output (in orange) to stimulate the mouse's hippocampus with a TTL signal sent from the digitizer to the laser for 50% of the events in a random manner (RND). Reproduced with permission.[95] Copyright 2013, The Authors. b) Wireless closed-loop optogenetics system across the entire dorsoventral spinal cord, including a pair of wires in specific muscles to record EMG signals, coupled with photostimulation. A tablet interface provides real-time display of these signals and photostimulation events, and offers the flexibility to configure algorithms for closed-loop operations. The image below illustrates the conditioned recording of tibialis anterior activity, which involves processes such as bandpass filtering, mains interference suppression, and down-sampling. Reproduced with permission.[94] Copyright 2021, The Authors, Springer Nature, America.

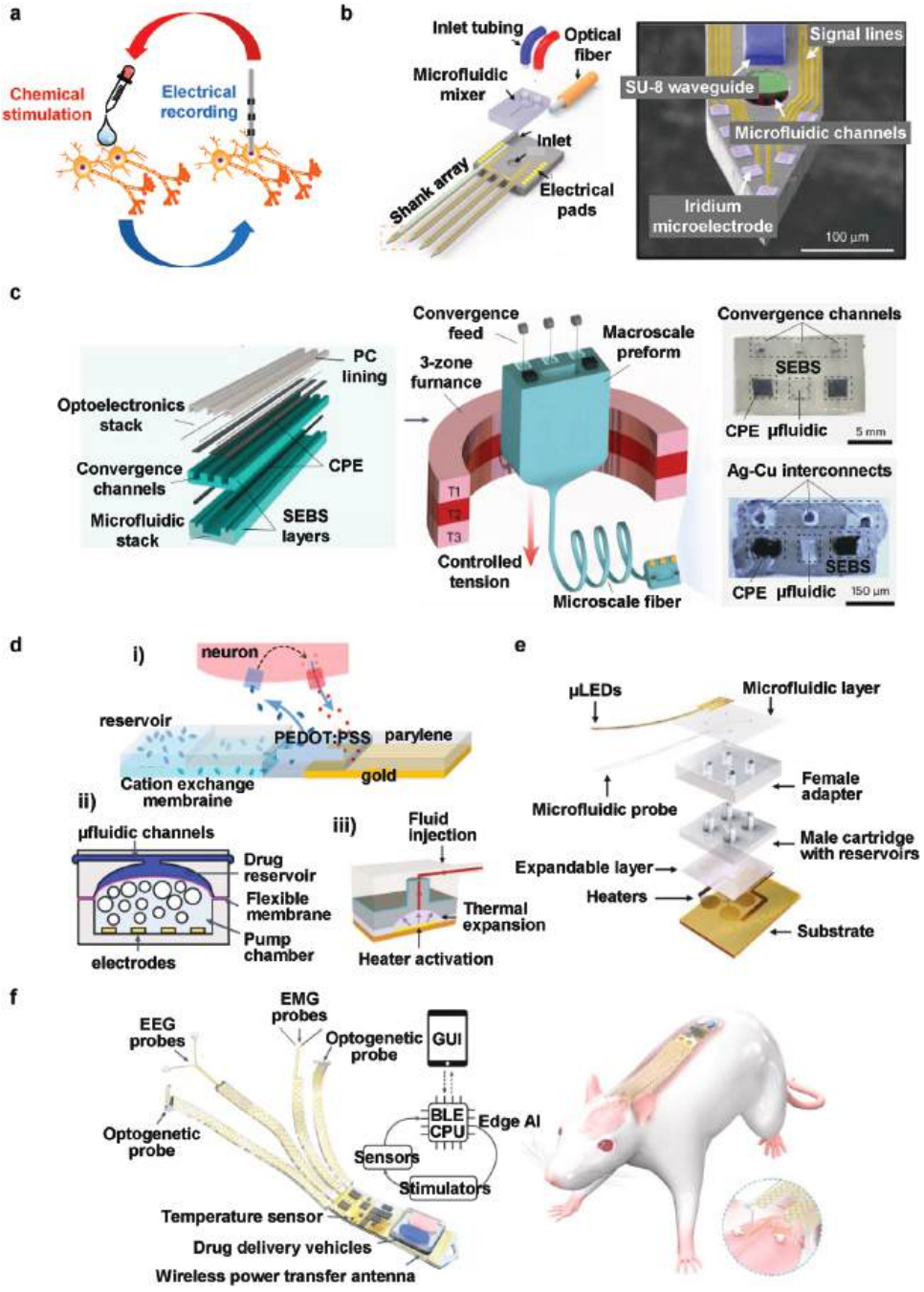

Figure 8. a) Closed-loop system with electrochemical sensing and multimodal stimulation. b) Schematic diagram (left) and image (right) of a multishank MEMS neural probe with a waveguide for optical stimulation, fluidic channels for drug delivery, and microelectrodes for electrophysiological recording. Reproduced with permission.[101] Copyright 2019, The Authors. c) Fabrication process and intersectional images of multifunctional fibrous neural probes, with carbon-doped polyethylene (CPE) as electrodes and interconnects, a hollow channel as microfluidic channel, and µLEDs as light source. Reproduced with permission.[110] Copyright 2023, The Authors. d) Structures and mechanisms of pumps of different principles for wireless drug delivery. i) Electrophoretic ion pump. The drug in the reservoir drifts out of the selective membrane to the neuron when voltage is applied on the nearby electrode. Reproduced with permission.[111] Copyright 2016, National Academy of Science. ii) Electrochemical pump. Gas generated by water electrolysis expands the chamber to pump out the drug into the reservoir. Reproduced with permission.[99] Copyright 2023, The Authors, under exclusive license to Springer Nature Limited. iii) Thermally actuated pump. Thermal expansion of a thermoresponsive polymer triggered by a Joule heater pumps out the drug into the reservoir. Reproduced with permission.[115] Copyright 2019, The Authors, under exclusive license to Springer Nature Limited. e) Structure of a tetherless neuromodulation unit with integrated pump and switchable drug reservoir. Reproduced with permission.[115] Copyright 2019, The Authors, under exclusive license to Springer Nature Limited. f) Wireless multimodal neuromodulation device with optogenetic stimulation, electrophysiological recording, temperature sensing, and closed-loop-controlled drug delivery functionalities. Reproduced with permission.[99] Copyright 2023, The Authors, under exclusive license to Springer Nature Limited.

bonding of an etched silicon trench and a cover wafer. Recording electrodes were then fabricated on the cover wafer. This process includes a 1050 °C heating procedure, which limits the application of the method. The same research group[106] used SiO_2 deposited by plasma-enhanced chemical vapor deposition (PECVD) to cover a trench and fabricated electrodes on an oxide layer. An optical fiber was also integrated to obtain a multifunctional device with electrophysiological recording, optical stimulation, and drug delivery functionalities. This device was implanted into the brains of rats, accomplishing neural recording when the drug was injected through the microchannels. The device functions for at least nine weeks after implantation and has the potential to achieve closed-loop modulation. A similar PECVD-based strategy was used by Pongrácz et al.[107] and an as-fabricated 380-µm thick, 400-µm wide multifunctional probe was used to record neural activities in the neocortex and thalamus of rats. Microfluidic channels can also be made completely from a negative photoresist using multiple photocuring cycles to define its shape. Frey et al.[108] fabricated the bottom, walls and cover of microfluidic channels by photocuring SU-8 photoresist three times. The as-fabricated channel was attached to a glutamate-sensing electrode array to form a neural probe. Neural probes made by microfabrication methods have well-defined microfeatures, though the fabrication procedure is relatively complicated and time-consuming.

In addition to microfabrication methods, thermal drawing is another method for fabricating neural probes with built-in microfluidic channels integrated with electrodes. As a traditional method of optical fiber production, thermal drawing is suitable for fabricating multifunctional neural probes and has the potential for scalable fabrication for its higher efficiency. Anikeeva et al. used thermal drawing to fabricate a series of multifunctional polymeric fibers with waveguide/light sources, electrodes, and microfluidic channels[66,109,110] (Figure 8c). These fibers are drawn from a structured preform obtained by rolling (cylindrical fibers) or stacking (rectangular fiber) layers of polymers with different properties. Conductive materials such as CPE are used conventionally and polycarbonate (PC) and COC are used often as waveguides and fluidic channel walls. These fibers have been used in simultaneous recording and optogenetic stimulation, recording and pharmacological stimulation, all-in-one optogenetics, pharmacological modulation of optogenetics, studying projections between brain regions, and interrogating gut–brain communication. These multifunctional fiber-integrated neuromodulation units have the potential to achieve closed-loop modulation when an electrophysiological signal is used as feedback from the control units.

These devices require a connection to a back-end injection system to provide drugs, which significantly limits their application. To promote the practical application of such devices, tetherless implantable multifunctional neuromodulation units with built-in parts to restore or generate drugs are required. To address this problem, researchers have designed reservoirs for drug storage and micropumps for on-demand drug release. The conventionally used micropumps can be categorized into three types based on their principles, namely electrophoretic ion, electrochemical, and thermal pumps (Figure 8d). The electrophoretic pump comprises a drug-loaded compartment sealed with a selective membrane and an electrode at its side. When electrical potential is applied to the electrode, charged drugs (e.g., K^+, Ca^{2+}, acetylcholine, and GABA) drift out of the membrane under an electric field to the neurons. The delivery rate is at the magnitude of pmol s^{-1}.[111,112] A neural probe comprising an electrophoretic ion pump and recording electrodes has been implanted into the hippocampus of mice and achieved therapeutic inhibition of 4AP-induced seizure-like events (SLEs) through the release of GABA by pumping it out through the microchannel. The thermal pump comprises a Joule heater and a drug reservoir with a base made of a thermally expandable layer. The expandable layer is a composite of PDMS and commercial expandable microspheres. When heated using a Joule heater, the sheet expands and squeezes the drug out of the reservoir. The flow rate of the thermal pump is at a magnitude of µL min^{-1}.[113,114] Reports indicate that thermal pumps require a temperature higher than 60 °C to function with a proper flow rate; however, the expandable layer can be replaced by other thermoresponsive materials such as hydrogels to lower the critical temperature to a range of body temperatures.[115] Replaceable reservoirs can be designed for these pumps (Figure 8e), enabling the chronic service of tetherless drug delivery units, which were formerly restricted by the limited capacity of the reservoir.[115] The electrochemical pump relies on the electrolysis of water induced by electrodes. It comprises an electrode submerged in a chamber of water, with a drug reservoir beside it and separated from the chamber by a flexible membrane. During operation, a current is applied to the electrode, leading to the electrolysis of water and generation of gases. These actions increase the pressure in the chamber, pushing the flexible membrane to the side of the drug reservoir and pumping out the drug. The flow rate of an electrochemical pump is at a magnitude of µL min^{-1}.[116,117] Compared with thermal pumps, electrochemical pumps consume less power, weigh less, and induce a lower temperature increase. Tetherless implantable drug delivery systems have been developed based on electrochemical pumps.[116,117]

In addition to these micromachine-based pumps, stimuli-responsive materials can be used to trigger drug release. Responsive hydrogel-based drug delivery systems have been studied intensively,[118,119] and some have been combined with sensing systems to realize feedback-regulated delivery. Chen et al.[23, 120] used a temperature-sensitive polyvinyl alcohol (PVA) hydrogel to encapsulate SiO_2-carried dopamine and integrated it with a Joule heater. When heated to 37.5–43.5 °C, PVA hydrogel de-crosslinks and releases dopamine. This releasing unit was integrated with an electrochemical dopamine sensor and a controlling memristor, allowing dopamine-level-controlled dopamine release. Compared to micropumps, responsive materials have higher design flexibility, though they are limited in stability.

The designs discussed above can be used to obtain tetherless closed-loop neuromodulation devices for drug delivery and other recording, sensing, and stimulation functions. Rogers et al.[99] fabricated a wireless multifunctional neuromodulation platform capable of conducting electrophysiological recordings, temperature sensing, optogenetic stimulation, drug delivery, and closed-loop modulation using a single device (Figure 8f). This device comprises two optogenetic probes based on µLEDs, two recording electrodes, a commercial temperature sensor, two drug reservoirs with a microfluidic channel and an electrochemical pump, a controlling circuit based on a Bluetooth low-energy system-on-a-chip (BLE SoC), and a near field communication (NFC) an-

tenna for wireless power transfer. Closed-loop seizure management in rats was achieved using this device. To determine the onset of epileptic seizures, a deep learning model was trained and uploaded to the BLE SoC for neural signal pattern recognition and quantification based on electrophysiological data obtained by electrodes. When a seizure starts in rats and is recognized by the SoC, the pump switches on and midazolam (a drug for reducing seizures) is released. In the in vivo experiments, seizures were reduced after the release of the drug, and the drug was released only when a seizure started.

In conclusion, drug-based chemical stimulation has high chemical-specificity and well-defined modulation effects, though the drug refilling requirements should be taken into consideration in the design and application of these devices. Compared with closed-loop systems based on electrical and optical stimulation, those based on drug stimulation are particularly suitable for repeated acute diseases, such as epilepsy. They can accomplish timely medication upon seizures. However, more work needs to be done for achieving stable closed-loop control of on-demand drug release.

6. Electrical/optical Stimulation and Electrochemical Sensing

This section mainly discusses modulation devices capable of chemical-specific sensing, where the stimulation ends could be electrical or optical stimulation (**Figure 9a**). Photochemical and electrochemical procedures are the main mechanisms of sensing; however, as photometry is discussed in Section 5, this section focuses only on electrochemical sensing.

Closed-loop modulation systems with specific electrochemical sensing and electrical stimulation techniques have been developed. Fast-scan cyclic voltammetry (FSCV) can be used to achieve quick, real-time electrochemical sensing of neurotransmitters.[121,122] Mohseni et al.[121] fabricated an SoC for the closed-loop regulation of brain dopamine based on FSCV sensing of dopamine and feedback-controlled electrical stimulation using an implantable carbon-fiber microelectrode. On-the-fly chemometrics were integrated with sensing and stimulation to achieve an automatic chemostat, maintaining the electrically evoked dopamine concentration between two set thresholds through on-off-keying (OOK) control (Figure 9b). The performance of the device was verified in vivo in the dorsal striata of rats.

Although closed-loop control has been achieved using chemical sensing devices, the control performance remains limited by the specificity and selectivity of the integrated chemical sensor. Additional fabrication and material strategies could be applied for the future development of chemical-specific closed-loop devices (introduced later).

Microfabrication methods are used frequently to fabricate state-of-the-art neuromodulation devices with electrochemical sensing functionalities. The microfabricated electrodes are chemically decorated afterward and can respond to specific neurochemicals. In decoration design, semipermeable membranes are used conventionally to prevent interference from reactions at the electrodes and enhance selectivity. Tooker et al.[123] fabricated a neural probe with electrodes and microfluidic channels and coated two electrodes with semipermeable membranes for amperometric dopamine sensing (Figure 9c). Sensing is based on the electrochemical oxidation of dopamine on the electrodes, and the coating prevents reductants other than dopamine from reaching the electrodes. The coating comprises a layer of over-oxidized polypyrrole (OPPy) and a Nafion layer, both of which are permselective cation polymers. Electrodeposition was employed for OPPy coating and electrochemical overoxidation, whereas Nafion was coated through dip coating. The dopamine sensing capability of this probe was tested in vitro, and its electrical recording and stimulation capabilities were tested in the basolateral amygdala (BLA) and mPFC. Garrett et al.[124] fabricated a multifunctional electrode for amperometric dopamine and uric acid sensing, electrical recording, and electrical stimulation, in which a nitrogen-containing ultra-nanocrystalline diamond membrane was used as the electrode coating. Its biosensing functionality was tested in vitro, and electrical interrogation in the retina of rats and in the visual cortex of wallabies. Coating semipermeable membrane is a simple way to endow probe with sensitivity to specific species, but its selectivity is still limited.

Biorecognition processes based on enzymes, antibodies, or aptamers can be used to further enhance selectivity. In a study reporting a probe with both electrochemical sensing and drug delivery functionalities, Frey et al.[125] decorated microfabricated electrodes with the enzyme choline oxidase (ChoOx) and a semipermeable membrane *m*-polyphenylenediamine (*m*-PPD) to make them selectively sensitive to choline (Figure 9d). ChoOx catalyzes the enzymatic oxidation of choline to generate hydrogen peroxide, which can be oxidized electrochemically at a certain voltage on sensing electrodes for amperometric measurements. ChoOx was immobilized on a glutaraldehyde(GA)-crosslinked bovine serum albumin (BSA) membrane coated on electrodes through electrochemically aided absorption. Semipermeable membranes reject certain electro-oxidizable interferents such as ascorbic acid and dopamine, which are coated by electrochemical polymerization. The choline sensing and drug delivery capabilities of this probe were verified using a brain phantom. The same research group developed a similar probe[108] for glutamate sensing and drug delivery by replacing ChoOx with L-glutamate oxidase (GluOx). Sensors modified with biorecognition agents have promoted selectivity, but the interaction between electrochemical sensing and stimulation still needs further optimization.

In addition to chemical interference, signal crosstalk is another challenge encountered by electrochemical probes. In the aforementioned studies, nonelectrical drug delivery was used for stimulation, or electrical stimulation and electrochemical sensing were separated temporally to avoid interference from signal crosstalk. Employing optical stimulation instead of electrical stimulation is another strategy for alleviating this issue. Sheng and coworkers[126] designed a neural probe with dopamine amperometric sensing and optogenetic stimulation functionalities. A PEDOT:PSS electrode was used as dopamine sensor, whereas an indium gallium nitride (InGaN)-based μLED was used as light source. To minimize interference from the driving current of μLED and prevent further occlusion of light transmission, a transparent and insulate polycrystalline diamond film was placed between the electrode and μLED (Figure 9). Owing to the photoelectric effect of the electrode, light could still affect the

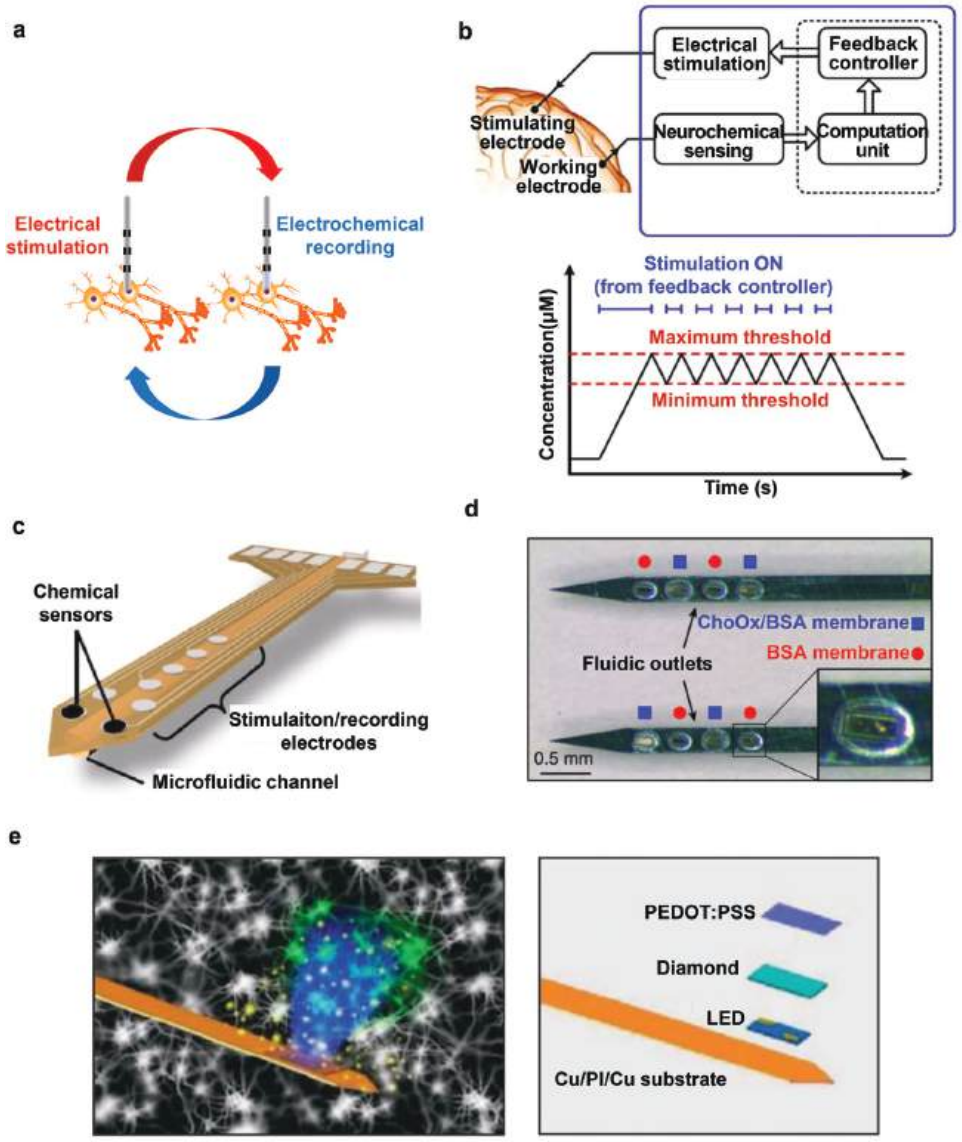

Figure 9. a) Multimodal neural recording and stimulation devices with electrochemical sensing functionality. b) Block diagram of closed-loop dopamine regulation of a neuromodulation system. Reproduced with permission.[121] Copyright 2015, IEEE. c) Structure of a bi-directional probe, 2 electrodes of which was coated by permselective membrane for dopamine electrochemical sensing. Reproduced with permission.[123] Copyright 2013 IEEE. (d) Image of a bi-directional probe with microfluidic channels and electrodes decorated with enzyme choline oxidase for choline electrochemical sensing. Reproduced with permission.[125] Copyright 2011, IOP Publishing Ltd. (e) Structure of a neural probe with optical stimulation and electrochemical dopamine detection functionalities. A polycrystalline diamond film was used to minimize interference from stimulation to sensing. Reproduced with permission.[126] Copyright 2020, The authors.

electrochemical sensing signal; however, this method can be developed further for orthogonal optical stimulation and biosensing.

To summarize, compared with electrical and optical sensing, electrochemical methods can achieve more specific monitoring of neural status, though they still face challenges like interferents. Another challenge comes from the coupling of stimulation and sensing when designing the closed-loop system. A stimulation signal that can precisely affects the level of the chemical of interest is needed, which requires more understanding of physiological procedures.

For chemical-specific closed-loop systems, as discussed in Sections 5 and 6, new accomplishments require more interdisciplinary effort for closed-loop neuromodulation devices with chemical interrogation functionalities. In addition to new materials and designs for chemical sensing and pharmacological stimulation methods, neural chemistry development for a new understanding of the functions of neurotransmitters, clinical medicine for new applications, control methods for closed-loop system construction, and machine learning for stimulation effect prediction can be used in this field. Abundant development has been achieved in chemical sensing and stimulation that have not been

used in closed-loop systems; therefore, combining this technique and those mentioned above to create new closed-loop devices is a promising approach.

From the viewpoint of materials and devices, the development of wireless and fully implantable devices is an emerging trend in neuromodulation, particularly for closed-loop modulation, of which the advantages outperform those of chronic applications. The reservoir-and-pump strategy is more suitable for these devices. To further prolong the lifetime of such devices, rechargeable reservoirs, such as those reported by Lee[104] are worth developing. To make pumps more biocompatible, stimuli-responsive materials for drug delivery, which have also been investigated intensively, can be used to replace microfabricated pumps. If drugs could be produced in situ using sources in a physiological environment, the convenience of closed-loop drug delivery could be enhanced further.

For devices with both electrochemical sensing and stimulation functionalities, avoiding interference from the stimulation line to the sensing line remains the most important challenge to solve before achieving simultaneous electrochemical sensing and stimulation, which requires new shielding materials and data processing algorithms. In addition, dopamine serves as a model analyte for numerous electrochemical sensors; however, few sensors targeting other important neurochemicals have been reported. Developing new selective methods for sensing other neurotransmitters is a meaningful direction in this field.

7. Ultrasound- and Magnetic-Based Interrogation in Closed-Loop Systems

In this section, we discuss the use of ultrasound and magnetic techniques in neuroscience research, as well as their applications and challenges in closed-loop neuromodulation systems (**Figure 10**a). Ultrasound and magnetic techniques are promising for neuroscience research. As a noninvasive strategy, focused ultrasound (FUS) has high spatial specificity and considerable penetration depth, making it a popular neuromodulation method. In particular, FUS in combination with microbubble-mediated therapy facilitates drug delivery across the blood–brain barrier (BBB) to treat many neural-related disorders.[127] In contrast with the traditional ablation of tissues caused by high-pressure ultrasound beams, microbubble monitoring utilizes the mechanical effects of bubble oscillations to reversibly adjust the BBB, which enables the delivery of large-molecule therapeutic drugs to target neural tissues. In addition, passive cavitation detection (PCD) can provide a controlled treatment approach using the Fourier spectra of the emission signals of microbubbles. In the case of PCD, the cavitation phenomenon in vessels can be divided into two categories, namely stable and inertial cavitation. Harmonic emission (HE) and broadband emission (BE) can reveal the strengths of stable and inertial cavitation, respectively.

The FUS-PCD based on a closed-loop system presents a cavitation emission-based control paradigm for modulating drug delivery through blood–brain barrier disruption (BBBD), using the cavitation result as the feedback signal to modulate stimulation. The core device of the system is shown in Figure 10b. Here BBBD was accomplished with the mechanical effect caused by ultrasound, and PCD was used to monitor the strength of ultrasound. The closed-loop system's feedback modulation step is arranged according to the PCD detection through a proportional–integral controller. This device is a dual-aperture FUS setup, with a central frequency of 274.3 kHz and a passive cavitation detector with a central frequency of 650 kHz. In this design, both apertures are driven by a small frequency shift to overcome the spatially homogenous BBBD caused by the interference pattern. For the feedback circuit, a proportional–integral controller is used to modulate the strength of the ultrasound stimulation. Performance characterization experiments show that HE displays highly linear behavior when expressed in decibels (dB) as a function of acoustic pressure. A series of optimization condition tests indicated that a microbubble dose of 200 μL kg^{-1} and pulse repetition frequency (PRF) of 4 Hz contributed optimal results. The correlation between the amount of tracer [Trypan Blue (TB)] and the integrated HE signal was investigated under optimal settings. The test was delivered to the striatum and hippocampus using different sonication durations, and the data displayed a correlation coefficient of up to 0.86, demonstrating the effectiveness of the PCD method. Experiments were conducted using a rat glioma model to validate the performance of the controllers. The tracers used were TB and liposomal doxorubicin (DOX)re. The F98 glioma cells were implanted at two bilateral sites in the striatum, and the magnetic resonance imaging (MRI) results showed that the ultrasound-treated area had BBBD and enhanced permeability of the blood–tumor barrier (BTB). Similarly, other studies have used the FUS-PCD technique to complete different tasks, such as inducing long-lived memory T cell formation within the brain that supports tumor rejection,[128] or validating the effective and safe FUS-induced BBB opening strategy in large animal models.[129]

Another alternative for addressing the challenge of drug delivery is magnetic resonance imaging-guided focused ultrasound (MRgFUS),[130] which differs from traditional ultrasound systems. The MRgFUS system was designed for localized trans-skull hyperthermia in rodents, employing thermosensitive liposomal Dox (TSL-Dox). The system was tested in two different glioma tumor models (F98 in rats and GL261 in mice). A schematic diagram of the experimental protocol used in this study is shown in Figure 10c. In the study, fluorescence microscopy was used to quantify and evaluate Dox delivery. The system operated at 1.7 MHz and, during work time, the brain-to-skull temperature ratio of the focus area reached the maximum level, maintaining it with high accuracy. Compared with the control group, an improvement of 3.5 times was observed in the cellular uptake in GL261 glioma mouse tumors and improvement of 5 times in F98 glioma rat tumors, validating the positive effects of the scheme.

Although many approaches to achieving closed-loop FUS-based modulation exist, reports on wearable ultrasound neuromodulation systems for potential human use are rare. Here, a general-purpose ultrasound neuromodulation system is proposed to make the device wearable.[131] In this study, a microelectromechanical system (MEMS)-based capacitive micromachined ultrasound transducer (CMUT) was developed. The CMUT contains multiple nanoscale capacitors, with top plates that can be actuated by the conversion of ultrasound energy caused by electrostatic energy and mechanical resonance. The ultrasound is sent to the transmission medium. The CMUT consists of 384 microchambers with an overall diameter of 8.1 mm. To enable

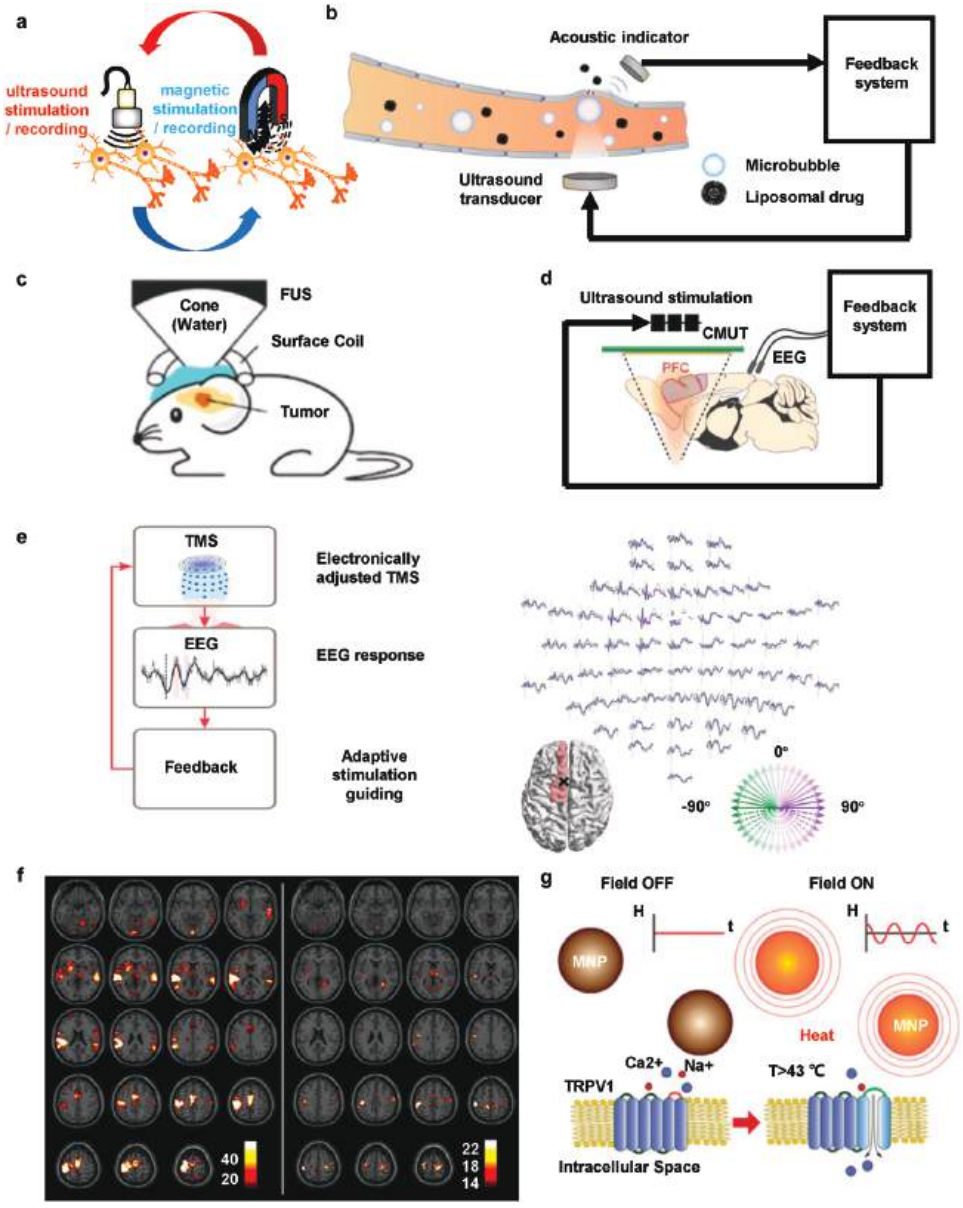

Figure 10. a) Closed-loop system with ultrasound or magnetic as stimulation and recording methods. b) Schematic of acoustic indicator and ultrasound transducer feedback controlled drug delivery system. Reproduced with permission.[127] Copyright 2017, Published under the PNAS license. c) Schematic of closed-loop trans-skull magnetic resonance imaging guided focused ultrasound system. Reproduced with permission.[130] Copyright 2021, Ivyspring International Publisher. d) Schematic of closed-loop ultrasound stimulation and EEG monitoring system. CMUT is short for chined ultrasound transducer. Reproduced with permission.[131] Copyright 2022, The Authors, Advanced Science published by Wiley-VCH GmbH. e) TMS-EEG closed-loop system and direction dependency test result of the TEPs on the pre-SMA. Reproduced with permission.[133] Copyright 2022, The Authors, published by Elsevier Inc. f) Activity in the primary motor cortex caused by voluntary thumb movements and the TMS effect. Reproduced with permission.[135] Copyright 2018, The Authors, Human Brain Mapping published by Wiley Periodicals, Inc. g) Magnetic field stimulation ("Field ON") of TRPV1 from MNP heating. Reproduced with permission.[136] Copyright 2015, American Association for the Advancement of Science.

resonance frequency of 460 kHz and 150 mW cm^{-2} ultrasound intensity, a direct wafer bonding process was adopted after dimensional analysis. The top electrode of each unit was made of gold (Au), the upper isolating layer was silicon (Si), the clapboard between two adjoining chambers was supported by silicon dioxide (SiO_2), and the device was encapsulated using a polydimethylsiloxane (PDMS)-parylene C bilayer passivation method. In this closed-loop ultrasound modulation setup, the ultrasound stimulation tool was integrated with EEG and EMG electrodes on a customized printed circuit board (PCB). The schematics of the closed-loop system are shown in Figure 10d. The CMUT device was packaged on the mice skull together with the electrodes to monitor the neuro activity situation during the four consecutive days of the experiment. The recorded data were analyzed and fed back to the stimulation controller to complete the real-time closed-loop modulation.

In addition to FUS applications, ultrasound technology can be used in ultrasound (US) imaging, incorporating other stimulation strategies to form a closed-loop neuromodulation system.[132] Peripheral electrical stimulation (ES) for tremor suppression in the upper limb can help treat neurological disorders such as Essential Tremor (ET), Parkinson's disease (PD), and dystonia. Sensing devices are required to reveal the stimulatory effect on muscle tissue. Moreover, a closed-loop-controlled stimulation system requires a method compatible with electrical stimulation. The US imaging provides an approach for direct visualization of the shallow and deep layers of the muscles. Further, US imaging is not affected by interference from nearby muscle signals and stimulus artifacts, displaying and identifying muscle tremors, or reflecting information about muscle contractility. Combined with wearable US transducers, this new approach is a promising closed-loop control technique.

Magnetic technology is another method of communicating neuronal activity. Popular magnetic technologies in the biomedical field include transcranial magnetic stimulation (TMS) and magnetic resonance imaging (MRI). In TMS, magnetic fields are used to stimulate neurons in the brain, whereas MRI creates images of the body using nuclear magnetic resonance (NMR). Magnetic methods display almost no side effects and have a wide range of applications. In addition, the TMS method can produce a direct causal effect on brain activity, which helps investigate the connections between different brain regions. Introducing magnetic techniques into a closed-loop neuromodulation system helps improve stimulation efficiency. Further, EEG measurements can provide parameter-adjusting feedback in an automated closed-loop TMS system, making it possible to use an optimized targeted stimulation mode, including the stimulation location and direction.[133] In this study, a multilocus TMS system and a two-coil transducer were adopted. Using these devices, a monophasic magnetic pulse could be applied to produce a biphasic electrical field at the stimulation position. Multilocus TMS can be modulated by applying stimulation in different directions to the target. The direction adjustment is based on the feedback EEG measurement results. BrainAmp DC (Brain Vision, LLC, North Carolina, USA) amplifiers were used for EEG signal recording. In the experiment, the sampling frequency was set to 5 kHz and the collected data were passed through a low-pass filter of 1 kHz. The left presupplementary motor area (pre-SMA) region was chosen as the test region. The contents of the test in this work include two aspects, namely the first test aimed to obtain the TMS-evoked potentials (TEPs) and stimulation relationship curve, and the second experiment is a feedback optimization test based on the TEP-stimulation function. A logical schematic is shown in the left side of Figure 10e. In the experiment, the TMS stimulation intensity was adjusted in different trials and a data visualization tool was used to assess the signal quality. If any large stimulation artifacts were found, the result was sent to the TMS stimulation controller for location adjustment according to the TEP-stimulation function. The right side of Figure 10e shows the direction-dependency test results for the TEPs on the pre-SMA. The black cross represents the position of the center of the transducer. Different colors indicate different stimulation directions and results. An artifact was used to reveal the stimulatory effect.

Several studies have suggested that transcranial electrical stimulation (tES) can be used to modulate target brain activity, and that functional MRI could be compatible with this method. This closed-loop method provides a new approach for treating brain-related neurological disorders. Mulyana et al. proposed a protocol concentrating on tES-fMRI closed-loop modulation optimization.[134] In this work, transcranial alternating current stimulation (tACS) was chosen as the form of tES. Considering the influence of MRI monitoring, a battery-driven MRI-compatible stimulation device was adopted, and measures of magnetic field isolation were designed to guarantee the quality of the results. Parameters such as frequency and phase difference were optimized in the frontal and parietal modulation processes. Furthermore, a closed-loop optimization protocol was presented.

Studies have shown that repetitive TMS of the left dorsolateral prefrontal cortex (DLPFC) could help treat major depressive disorder (MDD). However, the mechanism and changes in the target area after stimulation are unknown. A TMS-fMRI strategy provides an approach for recording and revealing the effects of TMS treatment.[135] In this method, a concurrent TMS-fMRI setting was used. The aim of the test was to study the influence of TMS-inducing activity on the left DLPFC area of healthy people, and fMRI technology was used to shed light on the stimulation process. The fMRI results recorded the direct effects of TMS as feedback of the closed-loop system. In these experiments, a Biphasic Magstim Rapid2 magnetic stimulator (Magstim Co. Ltd., UK) and an MR-compatible TMS coil were used. To reduce the interference between the stimulation and detection parts, a custom TMS filter box was arranged. One of the research aims was to compare the activity in the primary motor cortex caused by voluntary thumb movements with the TMS effect. The results showed strong similarities between voluntarily induced and TMS-induced brain activity, as shown in Figure 10f, demonstrating the effectiveness of the TMS treatment.

In addition to TMS and MRI techniques, other methods of magnetic regulation such as heat-sensitive strategies play an important role in minimally invasive remote neuromodulation. The approach using magnetic heating was based on the activation of the heat-sensitive capsaicin receptor TRPV1 using magnetic nanoparticles.[136] As shown in Figure 10g, these particles dissipate the heat generated by hysteresis, which triggers the firing of TRPV1+ neurons, thereby achieving neuromodulation. The nanoparticles were made from Fe_3O_4, with a diameter of 22 nm, and the highest heating rate per gram measured at a frequency of 500 kHz and a magnetic field strength H_0 of 15 kA m^{-1}. These magnetic nanoparticles were prepared by the thermal decomposition of a benign iron-oleate precursor and then dispersed in water after high-temperature ligand exchange. A layer of poly (ethylene glycol) chains covered the surface of the particles to improve their colloidal stability and biocompatibility. The magnetic nanoparticles were applied in wireless magnetothermal stimulation research on the ventral tegmental area of mice, displaying chronic stability.

Among the above-mentioned closed-loop neuromodulation schemes, the FUS-PVD-based closed-loop modulation strategy requires further improvements in the use of the cavitation phenomenon, and the portable closed-loop FUS systems should be validated in human treatments. Devices used for magnetic mod-

ulation are generally large and not conducive to miniaturization and portable use. Moreover, the specific magnetic modulation mechanisms should be further studied. In the future, we expect that portable systems suitable for clinical applications can be developed.

8. Conclusion

In summary, closed-loop control systems represent a crucial frontier in neuroscience research. The integration of multimodal stimulation and detection technologies has the potential to cure previously intractable neurological diseases in clinical settings, such as depression and Parkinson's disease, and even enable paralyzed patients to regain their mobility.[29,42] Furthermore, for closed-loop neuromodulation devices with multimodal stimulation and detection methods, new accomplishments require more interdisciplinary efforts that provide powerful tools for studying complex neural circuits.

Electric stimulation and modulation are currently the most mature and widely used technology in clinics, with the advantage of high temporal resolution, and it is developing into a more flexible and large-scale technology.[137] However, electrical stimulation is not cell-specific, meaning that it affects all cells within the stimulation range, limiting its efficacy in the study of complex brain circuitry. Optical methods combined with genetic modifications have gained advantages such as accuracy and specificity. These methods have unique advantages in the study of neural circuits and functions. Although electrical signals have long been recognized as crucial for neural signal transmission, it is important not to overlook the role of chemical signals, namely neurotransmitters, in mediating signal transmission between neurons. Therefore, the detection and stimulation of chemical signals constitute vital research directions for the study of neural circuits and neurological diseases. Furthermore, magnetic and ultrasound methods are promising noninvasive tools to study brain function at a large scale, which open new avenues in neuroscience research.

The closed-loop control technology shows a promising prospect for innovation in the medical field. Advances in technology and neuroscience are expected to offer new methods for the treatment of various chronic and neurological diseases.

Future research directions of closed-loop modulation system include multiple aspects. The first thrust is to provide deeper understanding of complex brain networks. This includes the exploration of brain network connectivity mechanisms, brain functional networks, and brain disease networks. It determines the effective extraction of biomarkers and the regulatory methods of the nervous system. In verse, its in-depth study really needs the participation of closed-loop systems. Therefore, the use of closed-loop modulation system for brain research is a trend in the future. In addition to the closed-loop regulation in CNS, the closed-loop regulation between CNS and PNS will also provide a powerful tool for us to better understand the complex brain networks and treat neurological diseases.[15] Second is the progress in the regulation of methods. In practical applications, choosing a system is often based on research or treatment objectives, available devices and technologies, characteristics of the studied neural network, and possible technical limitations. With technological developments, the advantages of each system could continue to strengthen, and new technologies could be integrated to combine such advantages. Such technology could achieve individualized closed-loop neural regulation that can potentially help researchers and medical practitioners to gain a deeper understanding of neural regulation. For example, if transcranial alternating current stimulation can be combined with synchronous recording of stereotactic electroencephalography (sEEG), changes in the local field potential intensity of deep neural nuclei under different current intensity stimuli (LFP) could be explored. Furthermore, if the optogenetic stimulation device is combined with magnetic resonance imaging, in vivo imaging of neuronal circuits during specific stimulation of a certain class of neurons can be achieved. Last is the improvement of deep learning algorithms. Although the focus of this review was on the hardware forming the closed-loop system, data processing and the recognition of collected signals, as well as the distribution of control signals require the participation of algorithms that play an important role in multimodal neural regulation and closed-loop regulation of stimuli. The identification of biomarkers is most important because the monitored signals are complex and have low signal-to-noise ratios. If machine learning can be applied to multimodal closed-loop control, it would significantly improve the monitoring efficiency of the technique.

While closed-loop neuromodulation holds immense promise, several challenges need to be addressed in the future. Firstly, suppressing the interference of stimulation signals on recorded signals remains the most important challenge, and optimization is required for device design, circuit functionality, and signal-processing algorithms. Secondly, closed-loop systems require multiple channels for recording and stimulation. These channels allow for comprehensive monitoring of neural signals and precise delivery of stimulation to specific brain regions or neural networks. Third, identification of relevant biomarkers is crucial for closed-loop systems., which related to the deep understanding of neural mechanism. What's more, advanced signal-processing techniques and machine learning algorithms could help detect specific neural markers associated with disease states or symptoms. Fourth, modern closed-loop systems often utilize wireless communication and reconfigurable platforms such as field-programmable gate arrays (FPGAs) or custom integrated circuits (ICs). These platforms enable flexibility and adaptability in real-time signal processing and the adjustment of stimulation parameters. Last but not least, to ensure patient safety, closed-loop systems incorporate safety mechanisms that continuously monitor adverse events, respond to emergencies, and provide failsafe features.

In summary, the development of a closed-loop control system should combine the strengths of the three fields of systems cybernetics, artificial intelligence, and brain science. Through interdisciplinary integration, more accurate decoding of data, more efficient stimulation intervention, and a more practical overall closed-loop system could be developed that play important roles in the diagnosis and treatment of clinical brain diseases.

Acknowledgements

This work was supported by National Natural Science Foundation of China (NSFC) (52272277, T2241026 to X.S), Beijing Municipal Natural Science Foundation (Z220015, to L.Y.), the China Postdoctoral Science Founda-

tion (2022M711765, to L.L.), the fellowship of China National Postdoctoral Program for Innovative Talents (BX20220170, to L.L), National Natural Science Foundation of China (NSFC) (82121003, to D.Y.)

Conflict of Interest

The authors declare no conflict of interest.

Keywords

closed-loop technique, neural sensing, neuromodulation

Received: September 27, 2023
Revised: March 11, 2024
Published online: April 30, 2024

[1] J. J. Jun, N. A. Steinmetz, J. H. Siegle, D. J. Denman, M. Bauza, B. Barbarits, A. K. Lee, C. A. Anastassiou, A. Andrei, Ç. Aydın, M. Barbic, T. J. Blanche, V. Bonin, J. Couto, B. Dutta, S. L. Gratiy, D. A. Gutnisky, M. Häusser, B. Karsh, P. R. Ledochowitsch, C. M. Lopez, C. Mitelut, S. Musa, M. Okun, M. Pachitariu, J. Putzeys, P. D. Rich, C. Rossant, W. Sun, K. Svoboda, et al., *Nature* **2017**, *551*, 232.
[2] Y. Wang, X. Yang, X. Zhang, Y. Wang, W. Pei, *Microsyst. Nanoeng.* **2023**, *9*, 1.
[3] T. H. Kim, M. J. Schnitzer, *Cell* **2022**, *185*, 9.
[4] Y. Dong, J. Li, M. Zhou, Y. Du, D. Liu, *Nat. Neurosci.* **2022**, *25*, 1675.
[5] J. Duyn, A. P. Koretsky, *Nat. Rev. Cardiol.* **2008**, *5*, S71.
[6] F. Zhang, L.-P. Wang, M. Brauner, J. F. Liewald, K. Kay, N. Watzke, P. G. Wood, E. Bamberg, G. Nagel, A. Gottschalk, K. Deisseroth, *Nature* **2007**, *446*, 633.
[7] K. Tybrandt, S. B. Kollipara, M. Berggren, *Sens. Actuators, B* **2014**, *195*, 651.
[8] M. Velliste, S. Perel, M. C. Spalding, A. S. Whitford, A. B. Schwartz, *Nature* **2008**, *453*, 1098.
[9] A. Jackson, J. Mavoori, E. E. Fetz, *Nature* **2006**, *444*, 56.
[10] H. Li, J. Wang, Y. Fang, *Microsyst. Nanoeng.* **2023**, *9*, 1.
[11] A. Vázquez-Guardado, Y. Yang, A. J. Bandodkar, J. A. Rogers, *Nat. Neurosci.* **2020**, *23*, 1522.
[12] R. Chen, A. Canales, P. Anikeeva, *Nat. Rev. Mater.* **2017**, *2*, 1.
[13] J. Rivnay, H. Wang, L. Fenno, K. Deisseroth, G. G. Malliaras, *Sci. Adv.* **2017**, *3*, e1601649.
[14] A. D. Mickle, S. M. Won, K. N. Noh, J. Yoon, K. W. Meacham, Y. Xue, L. A. McIlvried, B. A. Copits, V. K. Samineni, K. E. Crawford, D. H. Kim, P. Srivastava, B. H. Kim, S. Min, Y. Shiuan, Y. Yun, M. A. Payne, J. Zhang, H. Jang, Y. Li, H. H. Lai, Y. Huang, S. Park, R. W. Gereau 4th, J. A. Rogers, *Nature* **2019**, *565*, 361.
[15] D. Yao, Y. Qin, Y. Zhang, *Brain-Appar. Commun.: J. Bacomics* **2022**, *1*, 66.
[16] P. N. Banerjee, D. Filippi, W. A Hauser, *Epilepsy Res.* **2009**, *85*, 31.
[17] D. Schmidt, *Epilepsy Behav.* **2009**, *15*, 56.
[18] M. Vidailhet, L. Vercueil, J.-L. Houeto, P. Krystkowiak, A.-L. Benabid, P. Cornu, C. Lagrange, S. Tézenas du Montcel, D. Dormont, S. Grand, S. Blond, O. Detante, B. Pillon, C. Ardouin, Y. Agid, A. Destée, P. Pollak, *N. Engl. J. Med.* **2005**, *352*, 459.
[19] A. Schulze-Bonhage, *Seizure* **2017**, *44*, 169.
[20] R. S. Fisher, A. L. Velasco, *Nat. Rev. Neurol.* **2014**, *10*, 261.
[21] B. R. Voges, F. C. Schmitt, W. Hamel, P. M. House, C. Kluge, C. K. E. Moll, S. R. Stodieck, *Epilepsia* **2015**, *56*, e99.
[22] A. T. Connolly, A. Muralidharan, C. Hendrix, L. Johnson, R. Gupta, S. Stanslaski, T. Denison, K. B. Baker, J. L. Vitek, M. D. Johnson, *J. Neural Eng.* **2015**, *12*, 066012.
[23] B. Lee, M. N. Zubair, Y. D. Marquez, D. M. Lee, L. A. Kalayjian, C. N. Heck, C. Y. Liu, *World Neurosurg.* **2015**, *84*, 719.
[24] V. Kremen, B. H. Brinkmann, I. Kim, H. Guragain, M. Nasseri, A. L. Magee, T. Pal Attia, P. Nejedly, V. Sladky, N. Nelson, S. Chang, J. A. Herron, T. Adamski, S. Baldassano, J. Cimbalnik, V. Vasoli, E. Fehrmann, T. Chouinard, E. E. Patterson, B. Litt, M. Stead, J. V. Gompel, B. K. Sturges, H. J. Jo, C. M. Crowe, T. Denison, G. A. Worrell, *IEEE J. Transl. Eng. Health Med.* **2018**, *6*, 1.
[25] F. T. Sun, M. J. Morrell, R. E. Wharen, *Neurotherapeutics* **2008**, *5*, 68.
[26] P. E. Holtzheimer, M. M. Husain, S. H. Lisanby, S. F. Taylor, L. A. Whitworth, S. McClintock, K. V. Slavin, J. Berman, G. M. McKhann, P. G. Patil, B. R. Rittberg, A. Abosch, A. K. Pandurangi, K. L. Holloway, R. W. Lam, C. R. Honey, J. S. Neimat, J. M. Henderson, C. DeBattista, A. J. Rothschild, J. G. Pilitsis, R. T. Espinoza, G. Petrides, A. Y. Mogilner, K. Matthews, D. Peichel, R. E. Gross, C. Hamani, A. M. Lozano, H. S. Mayberg, *Lancet Psychiatry* **2017**, *4*, 839.
[27] D. D. Dougherty, A. R. Rezai, L. L. Carpenter, R. H. Howland, M. T. Bhati, J. P. O'Reardon, E. N. Eskandar, G. H. Baltuch, A. D. Machado, D. Kondziolka, C. Cusin, K. C. Evans, L. H. Price, K. Jacobs, M. Pandya, T. Denko, A. R. Tyrka, T. Brelje, T. Deckersbach, C. Kubu, D. A. Malone Jr, *Biol. Psychiatry* **2015**, *78*, 240.
[28] I. O. Bergfeld, M. Mantione, M. L. C. Hoogendoorn, H. G. Ruhé, P. Notten, J. van Laarhoven, I. Visser, M. Figee, B. P. de Kwaasteniet, F. Horst, A. H. Schen, P. v. d. Munckhof, G. Beute, R. Schuurman, D. Denys, *JAMA Psychiatry* **2016**, *73*, 456.
[29] K. W. Scangos, A. N. Khambhati, P. M. Daly, G. S. Makhoul, L. P. Sugrue, H. Zamanian, T. X. Liu, V. R. Rao, K. K. Sellers, H. E. Dawes, P. A. Starr, A. D. Krystal, E. F. Chang, *Nat. Med.* **2021**, *27*, 1696.
[30] W. Kang, C. Ju, J. Joo, J. Lee, Y.-M. Shon, S.-M. Park, *Nat. Commun.* **2022**, *13*, 7805.
[31] U. Topalovic, S. Barclay, C. Ling, A. Alzuhair, W. Yu, V. Hokhikyan, H. Chandrakumar, D. Rozgic, W. Jiang, S. Basir-Kazeruni, S. L. Maoz, C. S. Inman, M. Stangl, J. Gill, A. Bari, A. Fallah, D. Eliashiv, N. Pouratian, I. Fried, N. Suthana, D. Markovic, *Nat. Neurosci.* **2023**, 1.
[32] A. Zhou, S. R. Santacruz, B. C. Johnson, G. Alexandrov, A. Moin, F. L. Burghardt, J. M. Rabaey, J. M. Carmena, R. Muller, *Nat. Biomed. Eng.* **2019**, *3*, 15.
[33] A. Beuter, J.-P. Lefaucheur, J. Modolo, *Clin. Neurophysiol.* **2014**, *125*, 874.
[34] S. Kim, S. Kang, J. Kim, D. Lee, S. Kim, J. Lee, K.-I. Jang, Y.-S. Oh, J.-C. Rah, M. S. Huh, S. H. Paek, J. Choi, *IEEE Trans. Mol. Biol. Multiscale Commun.* **2021**, *7*, 209.
[35] A. Velisar, J. Syrkin-Nikolau, Z. Blumenfeld, M. H. Trager, M. F. Afzal, V. Prabhakar, H. Bronte-Stewart, *Brain. Stimul.* **2019**, *12*, 868.
[36] S. Little, M. Beudel, L. Zrinzo, T. Foltynie, P. Limousin, M. Hariz, S. Neal, B. Cheeran, H. Cagnan, J. Gratwicke, T. Z. Aziz, A. Pogosyan, P. Brown, *J. Neurol. Neurosurg. Psychiatry* **2016**, *87*, 717.
[37] N. C. Swann, C. de Hemptinne, M. C. Thompson, S. Miocinovic, A. M. Miller, R. Gilron, J. L. Ostrem, H. J. Chizeck, P. A. Starr, *J. Neural Eng.* **2018**, *15*, 046006.
[38] M. Arlotti, S. Marceglia, G. Foffani, J. Volkmann, A. M. Lozano, E. Moro, F. Cogiamanian, M. Prenassi, T. Bocci, F. Cortese, P. Rampini, S. Barbieri, A. Priori, *Neurology* **2018**, *90*, e971.
[39] M. Rosa, M. Arlotti, S. Marceglia, F. Cogiamanian, G. Ardolino, A. D. Fonzo, L. Lopiano, E. Scelzo, A. Merola, M. Locatelli, P. M. Rampini, A. Priori, *Mov. Disord.* **2017**, *32*, 628.
[40] S. Little, E. Tripoliti, M. Beudel, A. Pogosyan, H. Cagnan, D. Herz, S. Bestmann, T. Aziz, B. Cheeran, L. Zrinzo, M. Hariz, J. Hyam, P. Limousin, T. Foltynie, P. Brown, *J. Neurol. Neurosurg. Psychiatry* **2016**, *87*, 1388.
[41] S. Little, A. Pogosyan, S. Neal, B. Zavala, L. Zrinzo, M. Hariz, T. Foltynie, P. Limousin, K. Ashkan, J. FitzGerald, *Ann. Neurol.* **2013**, *74*, 449.

[42] F. Sun, M. Morrell, *Neurotherapeutics* **2014**, *11*, https://doi.org/10.1007/s13311-014-0280-3.
[43] P. D. Ganzer, M. J. Darrow, E. C. Meyers, B. R. Solorzano, A. D. Ruiz, N. M. Robertson, K. S. Adcock, J. T. James, H. S. Jeong, A. M. Becker, M. P. Goldberg, D. T. Pruitt, S. A. Hays, M. P. Kilgard, R. L. Rennaker 2nd, *Elife* **2018**, *7*, e32058.
[44] N. Wenger, E. M. Moraud, S. Raspopovic, M. Bonizzato, J. DiGiovanna, P. Musienko, M. Morari, S. Micera, G. Courtine, *Sci. Transl. Med.* **2014**, *6*, 255ra133.
[45] J. L. Collinger, B. Wodlinger, J. E. Downey, W. Wang, E. C. Tyler-Kabara, D. J. Weber, A. J. McMorland, M. Velliste, M. L. Boninger, A. B. Schwartz, *Lancet* **2013**, *381*, 557.
[46] B. Wodlinger, J. Downey, E. Tyler-Kabara, A. Schwartz, M. Boninger, J. Collinger, *J. Neural Eng.* **2014**, *12*, 016011.
[47] S. N. Flesher, J. E. Downey, J. M. Weiss, C. L. Hughes, A. J. Herrera, E. C. Tyler-Kabara, M. L. Boninger, J. L. Collinger, R. A. Gaunt, *Science* **2021**, *372*, 831.
[48] M. Capogrosso, T. Milekovic, D. Borton, F. Wagner, E. M. Moraud, J.-B. Mignardot, N. Buse, J. Gandar, Q. Barraud, D. Xing, E. Rey, S. Duis, Y. Jianzhong, W. K. D. Ko, Q. Li, P. Detemple, T. Denison, S. Micera, E. Bezard, J. Bloch, G. Courtine, *Nature* **2016**, *539*, 284.
[49] R. van den Brand, J. Heutschi, Q. Barraud, J. DiGiovanna, K. Bartholdi, M. Huerlimann, L. Friedli, I. Vollenweider, E. M. Moraud, S. Duis, N. Dominici, S. Micera, P. Musienko, G. Courtine, *Science* **2012**, *336*, 1182.
[50] Y. Lee, Y. Liu, D.-G. Seo, J. Y. Oh, Y. Kim, J. Li, J. Kang, J. Kim, J. Mun, A. M. Foudeh, Z. Bao, *Nat. Biomed. Eng.* **2023**, *7*, 511.
[51] E. S. Boyden, F. Zhang, E. Bamberg, G. Nagel, K. Deisseroth, *Nat. Neurosci.* **2005**, *8*, 1263.
[52] O. Yizhar, L. E. Fenno, T. J. Davidson, M. Mogri, K. Deisseroth, *Neuron* **2011**, *71*, 9.
[53] L. Tian, S. A. Hires, T. Mao, D. Huber, M. E. Chiappe, S. H. Chalasani, L. Petreanu, J. Akerboom, S. A. McKinney, E. R. Schreiter, C. I. Bargmann, V. Jayaraman, K. Svoboda, L. L. Looger, *Nat. Methods* **2009**, *6*, 875.
[54] T. Kondo, R. Saito, M. Otaka, K. Yoshino-Saito, A. Yamanaka, T. Yamamori, A. Watakabe, H. Mizukami, M. J. Schnitzer, K. F. Tanaka, J. Ushiba, H. Okano, *Cell Rep.* **2018**, *24*, 2191.
[55] F. Sun, J. Zeng, M. Jing, J. Zhou, J. Feng, S. F. Owen, Y. Luo, F. Li, H. Wang, T. Yamaguchi, Z. Yong, Y. Gao, W. Peng, L. Wang, S. Zhang, J. Du, D. Lin, M. Xu, A. C. Kreitzer, G. Cui, Y. Li, *Cell* **2018**, *174*, 481.
[56] F. Sun, J. Zhou, B. Dai, T. Qian, J. Zeng, X. Li, Y. Zhuo, Y. Zhang, Y. Wang, C. Qian, K. Tan, J. Feng, H. Dong, D. Lin, G. Cui, Y. Li, *Nat. Methods* **2020**, *17*, 1156.
[57] A. C. F. Bergs, J. F. Liewald, S. Rodriguez-Rozada, Q. Liu, C. Wirt, A. Bessel, N. Zeitzschel, H. Durmaz, A. Nozownik, H. Dill, M. Jospin, J. Vierock, C. I. Bargmann, P. Hegemann, J. S. Wiegert, A. Gottschalk, *Nat. Commun.* **2023**, *14*, 1939.
[58] X. Li, *OEA* **2023**, *6*, 230086.
[59] Z. Qi, Q. Guo, S. Wang, M. Jia, X. Gao, M. Luo, L. Fu, *Opto-Electron. Adv.* **2022**, *5*, 210081.
[60] L. Li, L. Lu, Y. Ren, G. Tang, Y. Zhao, X. Cai, Z. Shi, H. Ding, C. Liu, D. Cheng, Y. Xie, H. Wang, X. Fu, L. Yin, M. Luo, X. Sheng, *Nat. Commun.* **2022**, *13*, 839.
[61] Z. Zhang, L. E. Russell, A. M. Packer, O. M. Gauld, M. Häusser, *Nat. Methods* **2018**, *15*, 1037.
[62] J. Zhang, R. N. Hughes, N. Kim, I. P. Fallon, K. Bakhurin, J. Kim, F. P. U. Severino, H. H. Yin, *Nat. Biomed. Eng.* **2023**, *7*, 499.
[63] L. Grosenick, J. H. Marshel, K. Deisseroth, *Neuron* **2015**, *86*, 106.
[64] C. K. Kim, A. Adhikari, K. Deisseroth, *Nat. Rev. Neurosci.* **2017**, *18*, 222.
[65] F. Zhang, V. Gradinaru, A. R. Adamantidis, R. Durand, R. D. Airan, L. de Lecea, K. Deisseroth, *Nat. Protoc.* **2010**, *5*, 439.
[66] A. Canales, X. Jia, U. P. Froriep, R. A. Koppes, C. M. Tringides, J. Selvidge, C. Lu, C. Hou, L. Wei, Y. Fink, P. Anikeeva, *Nat. Biotechnol.* **2015**, *33*, 277.
[67] P. Anikeeva, A. S. Andalman, I. Witten, M. Warden, I. Goshen, L. Grosenick, L. A. Gunaydin, L. M. Frank, K. Deisseroth, *Nat. Neurosci.* **2011**, *15*, 163.
[68] N. G. Laxpati, B. Mahmoudi, C.-A. Gutekunst, J. P. Newman, R. Zeller-Townson, R. E. Gross, *Front. Neuroeng.* **2014**, *7*.
[69] J. Lee, I. Ozden, Y.-K. Song, A. V. Nurmikko, *Nat. Methods* **2015**, *12*, 1157.
[70] K. Kim, M. Vöröslakos, J. P. Seymour, K. D. Wise, G. Buzsáki, E. Yoon, *Nat. Commun.* **2020**, *11*, 2063.
[71] R. Ramezani, Y. Liu, F. Dehkhoda, A. Soltan, D. Haci, H. Zhao, D. Firfilionis, A. Hazra, M. O. Cunningham, A. Jackson, T. G. Constandinou, P. Degenaar, *IEEE Trans. Biomed. Circuits Syst.* **2018**, *12*, 576.
[72] A. E. Mendrela, K. Kim, D. English, S. McKenzie, J. Seymour, G. Buzsáki, E. Yoon, *IEEE Biomed. Circuits Syst Conf.*, **2017**, 1–4.
[73] W. Lee, D. Kim, N. Matsuhisa, M. Nagase, M. Sekino, G. G. Malliaras, T. Yokota, T. Someya, *Proc. Natl. Acad. Sci. USA* **2017**, *114*, 10554.
[74] K. Y. Kwon, B. Sirowatka, A. Weber, W. Li, *IEEE Trans. Biomed. Circuits Syst.* **2013**, *7*, 593.
[75] D.-W. Park, S. K. Brodnick, J. P. Ness, F. Atry, L. Krugner-Higby, A. Sandberg, S. Mikael, T. J. Richner, J. Novello, H. Kim, D.-H. Baek, J. Bong, S. T. Frye, S. Thongpang, K. I. Swanson, W. Lake, R. Pashaie, J. C. Williams, Z. Ma, *Nat. Protoc.* **2016**, *11*, 2201.
[76] A. Yazdan-Shahmorad, C. Diaz-Botia, T. L. Hanson, V. Kharazia, P. Ledochowitsh, M. M. Maharbiz, P. N. Sabes, *Neuron* **2016**, *89*, 927.
[77] Y. U. Cho, J. Y. Lee, U.-J. Jeong, S. H. Park, S. L. Lim, K. Y. Kim, J. W. Jang, J. H. Park, H. W. Kim, H. Shin, H. Jeon, Y. M. Jung, I.-J. Cho, K. J. Yu, *Adv. Funct. Mater.* **2022**, *32*, 2105568.
[78] Y. Zhu, Y. Deng, P. Yi, L. Peng, X. Lai, Z. Lin, *Adv. Mater. Technol.* **2019**, *4*, 1900413.
[79] S. Ye, A. R. Rathmell, Z. Chen, I. E. Stewart, B. J. Wiley, *Adv. Mater.* **2014**, *26*, 6670.
[80] E. D. Jung, Y. S. Nam, H. Seo, B. R. Lee, J. C. Yu, S. Y. Lee, J.-Y. Kim, J.-U. Park, M. H. Song, *Electron. Mater. Lett.* **2015**, *11*, 906.
[81] J. Zhang, X. Liu, W. Xu, W. Luo, M. Li, F. Chu, L. Xu, A. Cao, J. Guan, S. Tang, X. Duan, *Nano Lett.* **2018**, *18*, 2903.
[82] D.-W. Park, A. A. Schendel, S. Mikael, S. K. Brodnick, T. J. Richner, J. P. Ness, M. R. Hayat, F. Atry, S. T. Frye, R. Pashaie, S. Thongpang, Z. Ma, J. C. Williams, *Nat. Commun.* **2014**, *5*, 5258.
[83] H. Kang, S. Jung, S. Jeong, G. Kim, K. Lee, *Nat. Commun.* **2015**, *6*, 6503.
[84] R. Green, M. R. Abidian, *Adv. Mater.* **2015**, *27*, 7620.
[85] A. F. Renz, J. Lee, K. Tybrandt, M. Brzezinski, D. A. Lorenzo, M. Cerra Cheraka, J. Lee, F. Helmchen, J. Vörös, C. M. Lewis, *Adv. Healthcare Mater.* **2020**, *9*, 2000814.
[86] M. Thunemann, Y. Lu, X. Liu, K. Kılıç, M. Desjardins, M. Vandenberghe, S. Sadegh, P. A. Saisan, Q. Cheng, K. L. Weldy, H. Lyu, S. Djurovic, O. A. Andreassen, A. M. Dale, A. Devor, D. Kuzum, *Nat. Commun.* **2018**, *9*, 2035.
[87] D. Kuzum, H. Takano, E. Shim, J. C. Reed, H. Juul, A. G. Richardson, J. de Vries, H. Bink, M. A. Dichter, T. H. Lucas, D. A. Coulter, E. Cubukcu, B. Litt, *Nat. Commun.* **2014**, *5*, 5259.
[88] Y. Qiang, P. Artoni, K. J. Seo, S. Culaclii, V. Hogan, X. Zhao, Y. Zhong, X. Han, P.-M. Wang, Y.-K. Lo, Y. Li, H. A. Patel, Y. Huang, A. Sambangi, J. S. V. Chu, W. Liu, M. Fagiolini, H. Fang, *Sci. Adv.* **2018**, *4*, eaat0626.
[89] K. M. Kelly, *Epilepsy Curr.* **2007**, *7*, 159.
[90] P. Kwan, M. J. Brodie, *N. Engl. J. Med.* **2000**, *342*, 314.

[91] B. Zaaimi, M. Turnbull, A. Hazra, Y. Wang, C. Gandara, F. McLeod, E. E. McDermott, E. Escobedo-Cousin, A. S. Idil, R. G. Bailey, S. Tardio, A. Patel, N. Ponon, J. Gausden, D. Walsh, F. Hutchings, M. Kaiser, M. O. Cunningham, G. J. Clowry, F. E. N. LeBeau, T. G. Constandinou, S. N. Baker, N. Donaldson, P. Degenaar, A. O'Neill, A. J. Trevelyan, A. Jackson, *Nat. Biomed. Eng.* **2022**, 1.
[92] J. T. Paz, T. J. Davidson, E. S. Frechette, B. Delord, I. Parada, K. Peng, K. Deisseroth, J. R. Huguenard, *Nat. Neurosci.* **2013**, *16*, 64.
[93] E. Krook-Magnuson, G. G. Szabo, C. Armstrong, M. Oijala, I. Soltesz, *eNeuro* **2014**, *1*, 14.
[94] E. Krook-Magnuson, C. Armstrong, M. Oijala, I. Soltesz, *Nat. Commun.* **2013**, *4*, 1376.
[95] C. Kathe, F. Michoud, P. Schönle, A. Rowald, N. Brun, J. Ravier, I. Furfaro, V. Paggi, K. Kim, S. Soloukey, L. Asboth, T. H. Hutson, I. Jelescu, A. Philippides, N. Alwahab, J. Gandar, D. Huber, C. I. D. Zeeuw, Q. Barraud, Q. Huang, S. P. Lacour, G. Courtine, *Nat. Biotechnol.* **2022**, *40*, 198.
[96] S. Ramirez, X. Liu, C. J. MacDonald, A. Moffa, J. Zhou, R. L. Redondo, S. Tonegawa, *Nature* **2015**, *522*, 335.
[97] S. M. Iyer, K. L. Montgomery, C. Towne, S. Y. Lee, C. Ramakrishnan, K. Deisseroth, S. L. Delp, *Nat. Biotechnol.* **2014**, *32*, 274.
[98] S. H. Yun, S. J. J. Kwok, *Nat. Biomed. Eng.* **2017**, *1*, 0008.
[99] W. Ouyang, W. Lu, Y. Zhang, Y. Liu, J. U. Kim, H. Shen, Y. Wu, H. Luan, K. Kilner, S. P. Lee, Y. Lu, Y. Yang, J. Wang, Y. Yu, A. J. Wegener, J. A. Moreno, Z. N. Xie, Y. Wu, S. M. Won, K. Kwon, C. Wu, W. Bai, H. Guo, T.-L. Liu, H. Bai, G. Monti, J. Zhu, S. R. Madhvapathy, J. Trueb, M. Stanslaski, et al., *Nat. Biomed. Eng.* **2023**, 1.
[100] H. J. Lee, Y. Son, J. Kim, C. J. Lee, E.-S. Yoon, I.-J. Cho, *Lab Chip* **2015**, *15*, 1590.
[101] H. Shin, Y. Son, U. Chae, J. Kim, N. Choi, H. J. Lee, J. Woo, Y. Cho, S. H. Yang, C. J. Lee, I.-J. Cho, *Nat. Commun.* **2019**, *10*, 3777.
[102] S. Elyahoodayan, C. Larson, A. M. Cobo, E. Meng, D. Song, *J. Neurosci Methods* **2020**, *336*, 108634.
[103] A. M. Cobo, C. E. Larson, K. Scholten, J. A. Miranda, S. Elyahoodayan, D. Song, V. Pikov, E. Meng, *J. Microelectromech. Syst.* **2019**, *28*, 36.
[104] K. Lee, J. He, R. Clement, S. Massia, B. Kim, *Biosens. Bioelectron.* **2004**, *20*, 404.
[105] K. Seidl, S. Spieth, S. Herwik, J. Steigert, R. Zengerle, O. Paul, P. Ruther, *J. Micromech. Microeng.* **2010**, *20*, 105006.
[106] K. Sharma, Z. Jäckel, A. Schneider, O. Paul, I. Diester, P. Ruther, *J. Neural Eng.* **2021**, *18*, 066013.
[107] A. Pongrácz, Z. Fekete, G. Marton, R. Fiáth, P. Fürjes, I. Ulbert, G. Battistig, *Proc. Eng.* **2012**, *47*, 281.
[108] O. Frey, T. Holtzman, R. M. McNamara, D. E. H. Theobald, P. D. van der Wal, N. F. de Rooij, J. W. Dalley, M. Koudelka-Hep, *Sens. Actuators, B* **2011**, *154*, 96.
[109] S. Park, Y. Guo, X. Jia, H. K. Choe, B. Grena, J. Kang, J. Park, C. Lu, A. Canales, R. Chen, Y. S. Yim, G. B. Choi, Y. Fink, P. Anikeeva, *Nat. Neurosci.* **2017**, *20*, 612.
[110] A. Sahasrabudhe, L. E. Rupprecht, S. Orguc, T. Khudiyev, T. Tanaka, J. Sands, W. Zhu, A. Tabet, M. Manthey, H. Allen, G. Loke, M.-J. Antonini, D. Rosenfeld, J. Park, I. C. Garwood, W. Yan, F. Z. Niroui, Y. Fink, A. Chandrakasan, D. V. Bohórquez, P. Anikeeva, *Nat. Biotechnol.* **2023**, 1.
[111] S. H. K. Jonson Amanda, A. J. W. Oguziyilke, L. Kergoat, J. Rivnay, D. Khodagholy, M. Berggren, C. Bernard, G. G. Malliaras, D. T. Simon, *Proc. Natl. Acad. Sci. USA* **2016**, *113*, 9440.
[112] C. M. Proctor, A. Slézia, A. Kaszas, A. Ghestem, I. del Agua, A.-M. Pappa, C. Bernard, A. Williamson, G. G. Malliaras, *Sci. Adv.* **2018**, *4*, eaau1291.
[113] J.-W. Jeong, J. G. McCall, G. Shin, Y. Zhang, R. Al-Hasani, M. Kim, S. Li, J. Y. Sim, K.-I. Jang, Y. Shi, D. Y. Hong, Y. Liu, G. P. Schmitz, L. Xia, Z. He, P. Gamble, W. Z. Ray, Y. Huang, M. R. Bruchas, J. A. Rogers, *Cell* **2015**, *162*, 662.
[114] K. N. Noh, S. I. Park, R. Qazi, Z. Zou, A. D. Mickle, J. G. Grajales-Reyes, K.-I. Jang, R. W. Gereau IV, J. Xiao, J. A. Rogers, J.-W. Jeong, *Small* **2018**, *14*, 1702479.
[115] R. Qazi, A. M. Gomez, D. C. Castro, Z. Zou, J. Y. Sim, Y. Xiong, J. Abdo, C. Y. Kim, A. Anderson, F. Lohner, S.-H. Byun, B. C. Lee, K.-I. Jang, J. Xiao, M. R. Bruchas, J.-W. Jeong, *Nat. Biomed. Eng.* **2019**, *3*, 655.
[116] Y. Zhang, A. D. Mickle, P. Gutruf, L. A. McIlvried, H. Guo, Y. Wu, J. P. Golden, Y. Xue, J. G. Grajales-Reyes, X. Wang, S. Krishnan, Y. Xie, D. Peng, C.-J. Su, F. Zhang, J. T. Reeder, S. K. Vogt, Y. Huang, J. A. Rogers, R. W. Gereau, *Sci. Adv.* **2019**, *5*, eaaw5296.
[117] Y. Wu, M. Wu, A. Vázquez-Guardado, J. Kim, X. Zhang, R. Avila, J.-T. Kim, Y. Deng, Y. Yu, S. Melzer, Y. Bai, H. Yoon, L. Meng, Y. Zhang, H. Guo, L. Hong, E. E. Kanatzidis, C. R. Haney, E. A. Waters, A. R. Banks, Z. Hu, F. Lie, L. P. Chamorro, B. L. Sabatini, Y. Huang, Y. Kozorovitskiy, J. A. Rogers, *Nat. Commun.* **2022**, *13*, 5571.
[118] S. M. Mirvakili, R. Langer, *Nat. Electron.* **2021**, *4*, 464.
[119] S. Mura, J. Nicolas, P. Couvreur, *Nat. Mater.* **2013**, *12*, 991.
[120] T. Wang, M. Wang, J. Wang, L. Yang, X. Ren, G. Song, S. Chen, Y. Yuan, R. Liu, L. Pan, Z. Li, W. R. Leow, Y. Luo, S. Ji, Z. Cui, K. He, F. Zhang, F. Lv, Y. Tian, K. Cai, B. Yang, J. Niu, H. Zou, S. Liu, G. Xu, X. Fan, B. Hu, X. J. Loh, L. Wang, X. Chen, *Nat. Electron.* **2022**, *5*, 586.
[121] B. Bozorgzadeh, D. R. Schuweiler, M. J. Bobak, P. A. Garris, P. Mohseni, *IEEE Trans. Biomed. Circuits Syst.* **2015**, *10*, 654.
[122] S.-Y. Chang, C. J. Kimble, I. Kim, S. B. Paek, K. R. Kressin, J. B. Boesche, S. V. Whitlock, D. R. Eaker, A. Kasasbeh, A. E. Horne, C. D. Blaha, K. E. Bennet, K. H. Lee, *J Neurosurg Case Lessons* **2013**, *119*, 1556.
[123] A. Tooker, T. E. Madsen, A. Yorita, A. Crowell, K. G. Shah, S. Felix, H. S. Mayberg, S. Pannu, D. G. Rainnie, V. Tolosa, *IEEE Eng. Med. Biol. Soc. Annu. Conf* **2013**, 5159.
[124] M. A. Hejazi, W. Tong, A. Stacey, A. Soto-Breceda, M. R. Ibbotson, M. Yunzab, M. I. Maturana, A. Almasi, Y. J. Jung, S. Sun, H. Meffin, J. Fang, M. E. M. Stamp, K. Ganesan, K. Fox, A. Rifai, A. Nadarajah, S. Falahatdoost, S. Prawer, N. V. Apollo, D. J. Garrett, *Biomaterials* **2020**, *230*, 119648.
[125] O. Frey, P. Van Der Wal, S. Spieth, O. Brett, K. Seidl, O. Paul, P. Ruther, R. Zengerle, N. De Rooij, *J. Neural Eng.* **2011**, *8*, 066001.
[126] C. Liu, Y. Zhao, X. Cai, Y. Xie, T. Wang, D. Cheng, L. Li, R. Li, Y. Deng, H. Ding, G. Lv, G. Zhao, L. Liu, G. Zou, M. Feng, Q. Sun, L. Yin, X. Sheng, *Microsyst. Nanoeng.* **2020**, *6*, 64.
[127] T. Sun, Y. Zhang, C. Power, P. M. Alexander, J. T. Sutton, M. Aryal, N. Vykhodtseva, E. L. Miller, N. J. McDannold, *Proc. Natl. Acad. Sci. USA* **2017**, *114*, E10281.
[128] H. Lee, Y. Guo, J. L. Ross, S. Schoen, F. L. Degertekin, C. Arvanitis, *Sci. Adv.* **2022**, *8*, eadd2288.
[129] C.-Y. Chien, L. Xu, C. P. Pacia, Y. Yue, H. Chen, *Sci. Rep.* **2022**, *12*, 16147.
[130] C. Kim, Y. Guo, A. Velalopoulou, J. Leisen, A. Motamarry, K. Ramajayam, M. Aryal, D. Haemmerich, C. Arvanitis, *Theranostics* **2021**, *11*, 7276.
[131] Y. Jo, S.-M. Lee, T. Jung, G. Park, C. Lee, G. H. Im, S. Lee, J. S. Park, C. Oh, G. Kok, H. Kim, S. Kim, B. C. Lee, G. S. B. Suh, S.-G. Kim, J. Kim, H. J. Lee, *Adv. Sci.* **2022**, *9*, 2202345.
[132] N. Sharma, X. Xue, A. Iyer, X. Jiang, D. Roque, *Curr. Opin. Biomed. Eng.* **2023**, *28*, 100484.
[133] A. E. Tervo, J. O. Nieminen, P. Lioumis, J. Metsomaa, V. H. Souza, H. Sinisalo, M. Stenroos, J. Sarvas, R. J. Ilmoniemi, *Brain Stimul.* **2022**, *15*, 523.
[134] B. Mulyana, A. Tsuchiyagaito, M. Misaki, R. Kuplicki, J. Smith, G. Soleimani, A. Rashedi, D. Shereen, T. O. Bergman, S. Cheng, H. Kim, S. Kim, B. C. Lee, G. S. B. Suh, S.-G. Kim, J. Kim, H. J. Lee, *Brain Behav.* **2022**, *12*, e2667.

[135] J. J. T. Vink, S. Mandija, P. I. Petrov, C. A. T. van den Berg, I. E. C. Sommer, S. F. W. Neggers, *Hum. Brain Mapp.* **2018**, *39*, 4580.
[136] R. Chen, G. Romero, M. G. Christiansen, A. Mohr, P. Anikeeva, *Science* **2015**, *347*, 1477.
[137] P. Le Floch, S. Zhao, R. Liu, N. Molinari, E. Medina, H. Shen, Z. Wang, J. Kim, H. Sheng, S. Partarrieu, W. Wang, C. Sessler, G. Zhang, H. Park, X. Gong, A. Spencer, J. Lee, T. Ye, X. Tang, X. Wang, K. Bertoldi, N. Lu, B. Kozinsky, Z. Suo, J. Liu, *Nat. Nanotechnol.* **2023**, 1.
[138] J. Liu, T.-M. Fu, Z. Cheng, G. Hong, T. Zhou, L. Jin, M. Duvvuri, Z. Jiang, P. Kruskal, C. Xie, Z. Suo, Y. Fang, C. M. Lieber, *Nat. Nanotechnol.* **2015**, *10*, 629.

Lizhu Li is an associate professor in the Sichuan Provincial Key Laboratory for Human Disease Gene Study and the Center for Medical Genetics, School of Life Science and Technology at University of Electronic Science and Technology of China, China. She received her bachelor and PhD degrees from University of Electronic Science and Technology of China and Tsinghua University, respectively. Her current research interests involve implantable micro- and nanoscale optoelectronic materials and devices to develop advanced optical neural interfaces for neuroscience research.

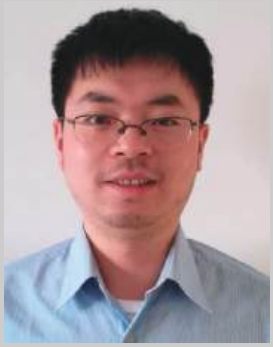

Xing Sheng is currently working as an associate professor in the Department of Electronic Engineering at Tsinghua University, China. He received his bachelor and PhD degrees from Tsinghua University and Massachusetts Institute of Technology, respectively. His current research is focused on advanced optoelectronic materials, devices and systems for biomedical applications.

Dezhong Yao is a professor in the Sichuan Provincial Key Laboratory for Human Disease Gene Study and the Center for Medical Genetics, School of Life Science and Technology at University of Electronic Science and Technology of China, China. He received his PhD degrees from Chengdu University of Technology. His current research is focused on multimodal imaging (EEG, MRI, and simultaneous EEG-fMRI) methods, Brain-Apparatus Communications (BAC) and their applications in aging and depression.